

Verifying Quantized Neural Networks using SMT-Based Model Checking

LUIZ SENA, Federal University of Amazonas, Brazil

XIDAN SONG, University of Manchester, United Kingdom

ERICKSON ALVES, Federal University of Amazonas, Brazil

IURY BESSA, Federal University of Amazonas, Brazil

EDOARDO MANINO, University of Manchester, United Kingdom

LUCAS CORDEIRO, University of Manchester, United Kingdom

Artificial Neural Networks (ANNs) are being deployed on an increasing number of safety-critical applications, including autonomous cars and medical diagnosis. However, concerns about their reliability have been raised due to their black-box nature and apparent fragility to adversarial attacks. Here, we develop and evaluate a symbolic verification framework using incremental model checking (IMC) and satisfiability modulo theories (SMT) to check for vulnerabilities in ANNs. More specifically, we propose several ANN-related optimizations for IMC, including invariant inference via interval analysis and the discretization of non-linear activation functions. With this, we can provide guarantees on the safe behavior of ANNs implemented both in floating-point and fixed-point (quantized) arithmetic. In this regard, our verification approach was able to verify and produce adversarial examples for 52 test cases spanning image classification and general machine learning applications. For small- to medium-sized ANN, our approach completes most of its verification runs in minutes. Moreover, in contrast to most state-of-the-art methods, our approach is not restricted to specific choices of activation functions or non-quantized representations.

Additional Key Words and Phrases: neural networks, verification

ACM Reference Format:

Luiz Sena, Xidan Song, Erickson Alves, Iury Bessa, Edoardo Manino, and Lucas Cordeiro. 2021. Verifying Quantized Neural Networks using SMT-Based Model Checking. *ACM Trans. Embedd. Comput. Syst.* 1, 1 (October 2021), 30 pages. <https://doi.org/10.1145/nnnnnnnn.nnnnnnnn>

1 INTRODUCTION

Artificial neural networks (ANNs) are soft computing models usually employed for regression, machine learning, and pattern recognition problems [11]. ANNs have been recently used to perform various safety-critical tasks. For instance, ANNs are employed for Covid-19 diagnosis [62], and for performing steering commands in self-driving cars [79]. Unfortunately, in such a context, incorrect classifications can cause serious problems. Indeed, adversarial disturbances can make

Authors' addresses: Luiz Sena, Federal University of Amazonas, Manaus, AM, Brazil, lhcs@icomp.ufam.edu.br; Xidan Song, University of Manchester, Manchester, United Kingdom, xidan.song@postgrad.manchester.ac.uk; Erickson Alves, Federal University of Amazonas, Manaus, AM, Brazil, erickson@icomp.ufam.edu.br; Iury Bessa, Federal University of Amazonas, Manaus, AM, Brazil, iurybessa@ufam.edu.br; Edoardo Manino, University of Manchester, Manchester, United Kingdom, edoardo.manino@manchester.ac.uk; Lucas Cordeiro, University of Manchester, Manchester, United Kingdom, lucas.cordeiro@manchester.ac.uk.

Permission to make digital or hard copies of all or part of this work for personal or classroom use is granted without fee provided that copies are not made or distributed for profit or commercial advantage and that copies bear this notice and the full citation on the first page. Copyrights for components of this work owned by others than ACM must be honored. Abstracting with credit is permitted. To copy otherwise, or republish, to post on servers or to redistribute to lists, requires prior specific permission and/or a fee. Request permissions from permissions@acm.org.

© 2021 Association for Computing Machinery.

1539-9087/2021/10-ART \$15.00

<https://doi.org/10.1145/nnnnnnnn.nnnnnnnn>

ANNs misclassify objects, thus causing severe damage to users of safety-critical systems. For instance, Eykholt *et al.* [26] showed that noise and disturbances, such as graffiti on traffic signals, could result in target misclassification during the operation of computer vision systems. Moreover, given that ANNs are notorious for being difficult to interpret and debug, the whole scenario becomes even more problematic [56], which then claims for techniques able to assess their structures and verify results and behaviors.

For this reason, there is a growing interest in the verification methods for ensuring the safety, accuracy, and robustness of neural networks. The approaches for verification of ANNs may be divided into three groups: optimization [27, 40, 68, 76], reachability [41, 46, 50, 75, 78, 81, 81] and satisfiability approaches [39, 43, 49, 61].

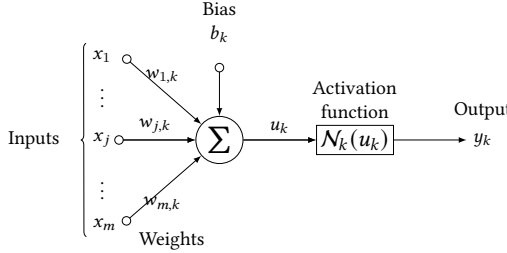
On the one hand, optimization-based algorithms pose the safety verification problem as an optimization problem, in which the safety properties are usually treated as constraints as described by Tjeng *et al.* [74]. The main difficulty of optimization methods, such as mixed-integer linear programming [12, 74, 76], branch and bound [68], and semi-definite programming [27], is to deal with the constraints that are non-linear and non-convex due to the network complex structure and its activation functions. It is still possible to employ dual optimization for simplifying those constraints and obtain a convex problem [25]; however, completeness tends to be lost due to the relaxations.

On the other hand, reachability-based approaches aim at computing the reachable sets of the ANNs by propagating the input sets through the network layer-by-layer while checking whether some unsafe state (violation) belongs or not to the reachable set. The main advantage of those methods is that they are usually sound, i.e., if the algorithm indicates that the network is unsafe, the safety property is violated. However, the computational cost to compute the exact reachable sets becomes unreasonable for more complex ANN's and more extensive input spaces. To avoid this problem, the reachable set is over-approximated by using symbolic [49, 50, 78] and/or set-theoretic methods [75, 81]. Although those tools effectively reduce the computational cost of the reachability sets, it is still challenging to over-approximate the ANNs non-linear elements, particularly the activation functions. There are some symbolic techniques to deal with the over-approximation of activation functions [41, 46]. However, most of the literature approaches are only able to approximate piecewise linear and ReLU activation functions.

Finally, satisfiability module theories encode both the ANN and the desired safety property into a single logic formula, and check whether a counterexample exists. In this regard, only binarized neural networks [44, 66] can be encoded in boolean logic and verified with existing SAT solvers [15, 61]. More complex ANN, whether implemented in floating-point or quantized to the integer domain for efficiency [51, 54], require the use of first-order logic. For these, several SMT-based approaches have been proposed [3, 32, 39, 43, 49, 50, 65]. While SMT background theories allow these approaches to model the semantic of the neural operations exactly, the resulting verification problem is challenging to solve [65]. In this respect, quantization has been proven to make the problem even harder computationally [39]. As a consequence, most existing approaches specialize in simple piecewise linear activation functions [3, 32, 49], focus on the floating-point scenario only [50] or require domain-specific abstractions [43].

Against this background, we propose a new approach to verify both fixed- and floating-point implementations of ANNs. Our main idea is to look at the source code of the ANN rather than the abstract mathematical model behind it. By doing this, we can leverage many recent advances in software verification that can dramatically increase the computational efficiency of the verification process.

More specifically, in this paper, we make the following original contributions:

Fig. 1. Detailed view of a single neuron n_k .

- We cast the ANN verification problem to a software verification problem. On the one hand, we propose a method to represent ANN safety properties as pairs of *assume* and *assert* instructions. On the other hand, we explain how to represent fixed- and floating-point operations in quantized ANN using operational models of their behavior.
- We introduce several pre-processing steps to increase the efficiency of the downstream software verification tools. Namely, we give a principled method to discretize non-linear activation functions and replace them with lookup tables. Furthermore, we show how to bound the feasible range of each variable with interval analysis and how to represent these bounds with additional *assume* instructions.
- We detail which existing techniques for search-space reduction can be borrowed from the software verification literature, and we empirically evaluate their individual and cumulative effects.
- We evaluate our approach on fixed- and floating-point ANNs and give empirical evidence on its computational efficiency. In particular, we show that we can verify ANNs with hundreds of neurons in less than an hour.

The remainder of this paper is structured in the following way. In Section 2, we introduce the ANN verification problem and present existing satisfiability modulo theories. In Section 3, we detail all the steps involved in our code-level verification approach for ANNs. In Section 4, we empirically test our approach on ANN classifiers trained on the classic Iris dataset and an image recognition dataset. In Section 5, we give a broader review of the recent trends in verifying ANNs. In Section 6 we conclude and outline possible future work.

2 PRELIMINARIES

Before introducing the details of our verification approach, let us review some important concepts related to the verification of artificial neural networks.

2.1 Artificial Neural Networks (ANNs)

Modern artificial neural networks (ANNs) are universal function approximators built by composing multiple copies of the same basic units, called neurons [11]. In their most common form, each neuron k is itself the composition of two functions as we illustrate in Fig. 1. The first is an affine projection of the m local inputs, often referred to as the *activation potential* u_k . The second is a non-linear transformation of the potential, often referred to as *activation function* N_k . Together, they define the following mapping $n_k : \mathbb{R}^m \rightarrow \mathbb{R}$:

$$y_k = N_k(u_k) \quad \text{where} \quad u_k(x) = \sum_{j=1}^m w_{j,k} x_j + b_k \quad (1)$$

The behavior of the basic neuron in Fig. 1 depends on the values of its weights w_k and on the activation function N_k . In this regard, researchers have experimented with a wide range of functions, including non-monotonic [63, 71], non-continuous [11], and unbounded ones [38, 60]. In our experiments of Section 4, we cover the most popular activation functions: namely, the rectified linear unit (ReLU), the sigmoid (Sigm), and its equivalent the hyperbolic tangent (TanH):

$$N_{\text{ReLU}}(u_k) = \max(0, u_k) \quad (2)$$

$$N_{\text{Sigm}}(u_k) = (1 + e^{-u_k})^{-1} \quad (3)$$

$$N_{\text{TanH}}(u_k) = 2N_{\text{Sigm}}(u_k) - 1 \quad (4)$$

At the same time, note that many state-of-the-art verification tools for ANNs are only compatible with ReLU and similar piece-wise linear activation functions [3, 32, 49]. Those that do support all activation functions [41, 46, 50] often incur a significant performance hit when solving the resulting non-linear verification problem. In contrast, the discretization technique we propose in Section 3.3 allows us to efficiently verify ANNs with any form of activation function.

Moreover, our verification methodology is general enough to be applied to a large variety of ANN architectures. Specifically, we support any feedforward, convolutional [53], recurrent [35], or graph neural network [80] that is built from the composition of the basic model of the neuron in Fig. 1. Similar to what has been reported in existing ANN verification studies [8, 43, 49], the primary factor influencing our verification time is the number of non-linearities in the neural network rather than its architecture (see Section 4).

2.2 Quantized Neural Networks (QNNs)

As the deployment of ANN in software applications becomes widespread, concerns about the power consumption of large models have increased. In this light, one of the main techniques to reduce the energy requirements of ANN inference is *quantization* [51], which replaces the floating-point operations required to compute the output of each neuron (see Equation 1) to integer [54] or even binary operations [44, 66]. State-of-the-art methods to perform such transformation significantly improve the low-power characteristics of ANNs while retaining the original predictive accuracy [37].

At the same time, the discretized nature of quantized neural networks (QNN) generates unique challenges regarding their verification [39]. More specifically, the output and intermediate computations performed by the network may differ from their floating-point counterparts. Thus, verification tools that operate on non-quantized ANN may return incorrect results.

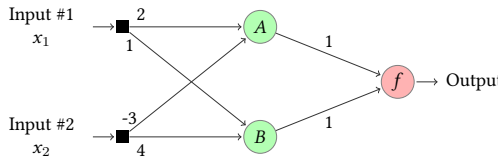


Fig. 2. Simple fully-connected neural network with ReLU activations and biases set to zero (not shown).

We demonstrate this with the following motivating example. Assume that we want to verify the neural network in Fig. 2, whose output can be directly computed as:

$$f(x_1, x_2) = A + B = \text{ReLU}(2x_1 - 3x_2) + \text{ReLU}(x_1 + 4x_2). \quad (5)$$

Furthermore, assume that in our example application, the output of the ANN must never fall below $f(x_1, x_2) \geq 2.7$, and that we want to verify whether this is true for the input $(x_1, x_2) = (0.749, 0.498)$.

Now, if we run the computation with infinite or 32-bit floating-point precision, the result is $f(0.749, 0.498) = 2.745$ which satisfies our safety property $f(x_1, x_2) \geq 2.7$. However, if the ANN has been quantized to a lower precision, this is not the case anymore. Indeed, for a QNN with 4-bit integer and 6-bit fractional precision, the output becomes $\hat{f}(0.749, 0.498) = 2.6867$, which violates our property. It is worth mentioning that such discrepancies can be even worse for larger ANNs, due to the accumulation of errors in the long computation chain. Thus, in our verification approach, we make sure to capture the actual operational model used in the ANN implementation (see Section 3.2).

2.3 Safety properties for ANNs and QNNs

Let us now formalize the concept of *safety property* we briefly mentioned in the previous Section 2.2. In general, a safety property defines the set of states that a system is designed to reach safely. In software verification, such properties are usually defined according to the user's domain knowledge, which allows them to state which program behaviors are safe [2]. In ANN verification, the black-box nature of the computation means that safety properties are usually defined on the inputs and outputs alone [42, 55]. In this paper, we often refer to safety properties in the following form:

$$x \in \mathcal{H} \implies f(x) \in \mathcal{G} \quad (6)$$

where x is an input vector and $f(x)$ is the corresponding output. Note however that our verification method supports any safety property that can be expressed in first-order logic (see Section 3.1).

A powerful and general way to define the input region \mathcal{H} is choosing a center point $x \in \mathcal{D}$ in the input domain \mathcal{D} , and letting the set $\mathcal{H}(x, d_{in})$ cover the whole neighborhood of points around it that are within a given distance $d_{in}(x, x') \leq 1$. For continuous input domains $\mathcal{D} \equiv \mathbb{R}^m$, such distance is often defined in terms of the family of p -norms as follows:

$$d_p(x, x') = \|x, x'\|_p = \left(\sum_{i=1}^m |x_i - x'_i|^p \right)^{\frac{1}{p}}, \quad \text{with } p \in [1, \infty) \quad (7)$$

where $p = 1$ is the Manhattan distance and $p = 2$ is the Euclidean distance. Furthermore, this definition can be extended to $p = \infty$ by introducing the so-called infinity or maximum norm $d_\infty(x, x') = \max_i(|x_i - x'_i|)$. Note that input regions defined through p_∞ can be described by a set of linear constraints, a fact that makes them attractive to the verification community for efficiency reasons [49, 70, 78]. Also, note that the input vectors can be rescaled using a diagonal matrix Z , allowing us to define hyper-ellipsoids (if $p = 2$) and hyper-rectangles (if $p = \infty$) in the input space:

$$\hat{d}_p(x, x', Z) = d_p(Zx, Zx') \quad (8)$$

A little more care is required if the input domain \mathcal{M} is discrete in nature, for instance, in natural language processing (NLP) applications. However, a mapping to a continuous space is often available [48].

Once we establish a definition for the input set \mathcal{H} in Equation 6, we can complete the definition of our safety property by choosing the corresponding output set \mathcal{G} [55]. For regression tasks, we can again define a safe neighborhood around an output point $f(x)$ within a given distance $d_{out}(f(x), f(x')) \leq 1, \forall x' \in \mathcal{H}(x, d_{in})$. For classification tasks, the output set \mathcal{G} often comprises all points that assign the highest score to the desired class, e.g. $\mathcal{G} \equiv \{y | (y = f(x), \forall x \in \mathcal{D}) \wedge (y_i > y_j, \forall j \neq i)\}$ for output class i . In Section 3.1 we show how to define this kind of safety properties inside our verification tool.

2.4 Satisfiability Modulo Theories (SMT)

Once we have defined a safety property P according to Equation 6, we need to verify that it always holds for our (quantized) neural network. As we mentioned in Section 1, there exist many approximate techniques to do so. However, in this paper, we focus on bit-precise verification via *satisfiability modulo theories* (SMT) solvers [7].

Similar to Boolean Satisfiability (SAT) solving [77], the SMT approach to verification works by converting the verification problem at hand into a logic formula and checking whether the said formula is satisfiable. However, SMT extends SAT beyond boolean logic and allows us to model the verification problem in a decidable subset of first-order logic. At the same time, the interpretation of these models is restricted to a combination of *background theories*, written in first-order logic with equality. More formally, given a first-order formula F encoding the verification problem and a background theory T , we say that F is T -satisfiable if and only if there exists an assignment such that the union $F \cup \{T\}$ is satisfiable.

The modeling power of SMT comes from the variety of background theories T that we can use. These theories model the semantic of common mathematical objects like real, floating-point, and integer numbers, arrays, lists, bit vectors, and the operations defined on them for computational problems [6]. While the modeling capabilities of SMT are still being extended to new domains (see e.g. [22]), mainstream SMT solvers (e.g., Z3 [21], CVC4 [4] and Boolector [13]) already offer native support for all of the theories above.

2.5 Existing SMT approaches for ANNs and QNNs

SMT approaches have been applied to an extensive range of verification problems [7]. In this section, we review existing approaches for ANNs and QNNs. Note that due to the SMT paradigm flexibility, these approaches vary in the abstraction level at which they tackle the verification problem.

Early research applied existing SMT solvers to the verification of real-valued ANNs and showed some difficulties in scaling beyond toy examples [65]. More recently, Katz *et al.* proposed to extend the background theory of real numbers and include an extra predicate for the ReLU activation function [49]. Since each ReLU doubles the number of verification formulas, they introduce a dedicated lazy solver, called Reluplex, that only visits the relevant subset of formulas. Their algorithm has been subsequently extended to all piecewise-linear activation functions [50]. An alternative approach by Huang *et al.* asks the user to define a problem-dependent set of micro-manipulations that the SMT solver can chain to search the state space [43]. With this approach, they can scale to medium-sized ANNs for image classification. Furthermore, verification approaches based on real number computation can be easily extended to cover floating-point implementations on ANNs [49, 70].

In contrast, SMT methods to verify QNNs have to contend with a more challenging computational problem from the theoretical perspective [39]. In this respect, Giacobbe *et al.* choose to represent the QNN operations with the bit-vector background theory and shows that the verification result can be very different from its real and floating-point counterparts [32]. Similarly, Baranowski *et al.* propose a new fixed-point background theory and test it on some small QNNs [3]. In general, low-level optimizations in the SMT encoding of the QNN are shown to speed up the verification process considerably [32, 39]. In the extreme case of binarized neural networks, where the quantization only allows two binary states for each variable, the verification problem reduces to SAT solving [61]. Here, hardware-level optimizations are crucial for efficiency too [15].

Our methodology is a generalization of the previous work by Sena *et al.* on the SMT verification of CUDA implementations of ANNs [69]. As we expound in the next Section 3, we take advantage of existing techniques in software verification to model both ANNs and QNNs as SMT formulas.

Our novelty lies in the encoding of fixed-point operations and the efficient treatment of non-linear activation functions, which allows us to verify networks beyond the simple ReLU function.

3 INCREMENTAL VERIFICATION OF NEURAL NETWORKS USING INVARIANT INFERENCE

While we usually think of neural networks as mathematical models, their implementation is written in code. Thus, in this respect, neural networks can be treated like any other piece of software. The advantage of this strategy is twofold. First, we can readily adapt many existing software verification techniques to ANNs and QNNs. Second, we give the user access to these highly technical verification tools in a familiar coding framework.

This section lists the sequence of steps required to verify ANNs in such way. To this end, we assume that the ANN is given as input in the form of a piece of C code, and the user specifies the desired safety property with `assume` and `assert` statements as detailed in Section 3.1. Likewise, we explain how to represent a quantized ANN by calling our finite-word length (FWL) operational models in Section 3.2.

With this input, our verification methodology unfolds in three steps. First, we discretize each activation function with the algorithm in Section 3.3. Second, we compute a reachable set of values for each variable with the invariant inference techniques in Section 3.4. Third, we verify the safety property via SMT model checking as explained in Section 3.5. All the techniques we use to reduce the search space of the SMT solver are listed in Sections 3.6 and 3.7.

We give a visual summary of our verification methodology in Figure 3. Furthermore, we walk through a complete example of our workflow in Section 3.8.

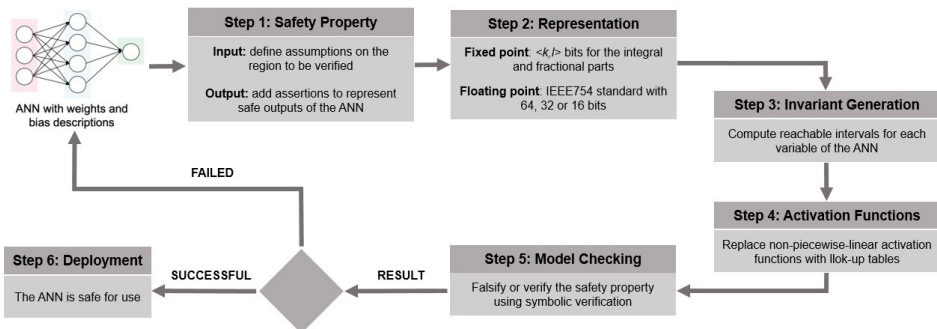


Fig. 3. Proposed verification methodology for fixed- and floating-point ANNs.

3.1 Introducing safety properties in the ANN code

As we explain in Section 2.3 verifying an ANN means proving that a given safety property holds. Such safety property is a falsifiable mathematical relation defined on the value of ANN variables. Since we are considering the software implementation of ANNs here, in this section, we show how to annotate the ANN code and specify the desired safety property.

Let us consider safety properties in the general form $x \in \mathcal{H} \implies y \in \mathcal{G}$, where knowing that the vector of variables x belongs to \mathcal{H} guarantees that the output vector $y = f(x)$ belongs to set \mathcal{G} . We encode the premise of the implication with the pre-condition instruction `assume`, specifying the set of values \mathcal{H} that each $x_i \in x$ can take. For example, a rectangular domain for the input variables $x_1 \in [0, 2]$ and $x_2 \in [-\frac{1}{2}, +\frac{1}{2}]$ can be encoded as follows:

$$\text{assume}(x_1 \geq 0 \ \&\& x_1 \leq 2) \quad (9)$$

$$\text{assume}(x_2 \geq -0.5 \ \&\& x_2 < 0.5) \quad (10)$$

This notation instructs the subsequent SMT model checking to search only the inputs that satisfy the conditions specified in the `assume` instruction, thus making sure that the premise of the safety property $x \in \mathcal{H}$ is satisfied. Note also that the instruction `assume` is general and supports any boolean expression as its argument. Thus, any form of input region \mathcal{H} can be specified, as long as it is valid C code syntax. At the same time, hyperrectangular input domains tend to lead to faster verification times.

In contrast, we encode the conclusion of the implication with the post-condition instruction `assert`, specifying the set of values \mathcal{G} that each variable $y_i \in y$ can safely range in. As an example, if we have a binary classification network with two outputs y_1, y_2 indicating the score of each class, we can encode the conclusion of a robustness safety property for class two as follows:

$$\text{assert}(y_2 > y_1) \quad (11)$$

Thus requiring that when the premise is satisfied, our binary network always predicts class two. As for the input region \mathcal{H} , the `assert` instruction can be used to specify a variety of output regions \mathcal{G} .

3.2 Operational models for fixed-point ANN implementations

In this section, we discuss how our operational model works to support fixed-point verification of neural network implementations.

Generally, there are two ways of supporting fixed-point neural network implementations [32]: (1) convert inputs to fixed-point and perform all the underlying steps, *e.g.*, training and validation, in fixed-point; and, (2) convert trained models and neural network operations, *e.g.*, realization, in floating-point representation to fixed-point and then check the desired properties. The former is likely to produce better representations, but the latter is likely to be more practical [45], especially since datasets are usually provided in floating-point representation. In this work, we have chosen the latter.

Our goal is to transform an existing model (and its constraints) defined in the C programming language into a fixed-point representation. Here, a fixed-point representation is specified as $\langle k, l \rangle$, where k denotes the number of bits to encode an integral part I and l the number of bits to encode a fractional part F . Furthermore, given a rational number, we can represent it in fixed-point by using $k + l$ bits and it is interpreted as $I + \frac{F}{2^l}$. Such representation allows us to take the hardware platform limitations, where the model will be executed, into account.

In order to model the effect of quantization on the ANN computation steps, we need to convert each arithmetic operation (addition, subtraction, multiplication, and division) from floating-point to their respective fixed-point counterparts. In particular, these operations and conversions must take into account the parameters k and l . We achieve this goal with the operational models proposed in [14], which have been extensively validated in the digital controller domain. Furthermore, these operational models formally define a set of methods and values that precisely represent fixed-point operations' behavior.

In Fig. 4 we show an example of how to convert a piece of floating-point source-code to a fixed-point representation with the proposed operational models. Here, we have a snippet of code that computes the activation potential of a single neuron, one of the basic operations in ANNs. Notice how the types and operations have been changed in the fixed-point version. In particular,

`fxp_float_to_fxp` transforms a `float` type to a `fpx_t` type, and both `fpx_add` and `fpx_mult` make sure that the addition and multiplication arithmetic operations are performed in fixed-point.

```

1 float potential(float *w,
2                 unsigned int w_len,
3                 float **x,
4                 unsigned int x_len,
5                 float b) {
6
7     if (w_len != x_len) {
8         return 0;
9     }
10
11    float result = 0;
12
13    for (unsigned int i = 0; i < w_len;
14        ++i) {
15        result += w[i] * x[i];
16    }
17
18    result += b;
19
20    return result;
}

```

```

1 fpx_t potential(float *w,
2                  unsigned int w_len,
3                  float **x,
4                  unsigned int x_len,
5                  float b) {
6
7     if (w_len != x_len) {
8         return 0;
9     }
10
11    fpx_t result = 0;
12    for (unsigned int i = 0; i < w_len;
13        ++i) {
14        fpx_t w_fxp = fxp_float_to_fxp(w[i]);
15        fpx_t x_fxp = fxp_float_to_fxp(x[i]);
16        result = fpx_add(result, fpx_mult(w_fxp, x_fxp));
17    }
18    fpx_t b_fxp = fxp_float_to_fxp(b);
19    result = fpx_add(result, b_fxp);
20    return result;
}

```

(a) Floating-point version

(b) Fixed-point version

Fig. 4. A method to compute the activation potential of neurons implemented in C.

In summary, the fixed-point version of the ANN code references the appropriate operational model, thus ensuring that the behavior of each fixed-point arithmetic operation is modeled correctly. We show the impact of different levels of granularity in the quantization of ANNs in our experiments in Sections 4.4 and 4.4.2.

3.3 Discretization of non-linear activation functions

As we mention in Section 2.1, the choice of activation function can have a considerable impact on the verification time. While piece-wise linear functions can be readily represented as a (sequence of) if-then-else instructions, non-linear activation functions require more care to avoid severe performance degradation. This section presents an approach to convert such non-linear functions into look-up tables, thus significantly speeding up the verification process.

Assume that the non-linear activation function $\mathcal{N} : \mathcal{U} \mapsto \mathbb{R}$ is a piece-wise Lipschitz continuous function, thus there is a finite set of a locally Lipschitz continuous functions $\mathcal{N}_i : \mathcal{U}_i \mapsto \mathbb{R}$ for $i \in \mathbb{N}_{\leq a}$, so-called selection functions, such that the sets $\mathcal{U}_i \subset \mathbb{R}$ are disjoint intervals, $\mathcal{N}(u) \in \{\mathcal{N}_1(u), \dots, \mathcal{N}_a(u)\}$ holds for all $u \in \mathbb{U}$, $\mathcal{U} = \bigcup_{i \in \mathbb{N}_{\leq a}} \mathcal{U}_i$, and

$$\|\mathcal{N}_i(u_1) - \mathcal{N}_i(u_2)\| \leq \lambda_i \|u_1 - u_2\|, \quad \forall u_1, u_2 \in \mathcal{U}_i, \quad (12)$$

where λ_i denotes the Lipschitz constant of \mathcal{N}_i .

The proposed discretisation approach is applied to each subset \mathcal{U}_i . The general idea consists in discretising the \mathcal{U}_i by obtaining the discrete and countable set $\tilde{\mathcal{U}}_i \subset \mathcal{U}_i$. Then, we build a lookup table for rounding the evaluation of $\mathcal{N}_i(u)$ to $\tilde{\mathcal{N}}_i(u) : \mathcal{U}_i \mapsto \mathcal{R}$, and consequently round $\mathcal{N}(u)$ to $\tilde{\mathcal{N}}(u) \in \{\tilde{\mathcal{N}}_1(u), \dots, \tilde{\mathcal{N}}_a(u)\}$. The lookup table contains uniformly distributed N_i samples within \mathcal{U}_i , including the interval limits, to ensure the accuracy $\|\tilde{\mathcal{N}}_i(u) - \mathcal{N}_i(u)\| \leq \epsilon$. Let L_i be defined as the length of the interval \mathcal{U}_i , i.e.

$$L_i \triangleq \sup_{u \in \mathcal{U}_i} u - \inf_{u \in \mathcal{U}_i} u. \quad (13)$$

The following Theorem can be used to choose the number of samples N_i to ensure the desired accuracy ϵ .

THEOREM 3.1. *Let the non-linear activation function $\mathcal{N} : \mathcal{U} \mapsto \mathbb{R}$, $\mathcal{N} \in \{\mathcal{N}_1(u), \dots, \mathcal{N}_a(u)\}$, be piecewise Lipschitz continuous such that each selection function $\mathcal{N}_i(u) : \mathcal{U}_i \mapsto \mathcal{R}$ presents the Lipschitz constant λ_i , and consider the discrete approximation $\tilde{\mathcal{N}}(u) \in \{\tilde{\mathcal{N}}_1(u), \dots, \tilde{\mathcal{N}}_a(u)\}$, where each selection function $\tilde{\mathcal{N}}_i : \mathcal{U}_i \mapsto \mathbb{R}$, for $i \in \mathbb{N}_{\leq a}$ is obtained with $\mathcal{U}_i \subset \mathcal{U}$ containing N_i samples. The approximation error is bounded as*

$$\|\tilde{\mathcal{N}}(u) - \mathcal{N}(u)\| \leq \epsilon, \quad (14)$$

for a given ϵ , if the following conditions hold

$$N_i \geq 1 + \frac{L_i \lambda_i}{\epsilon}, \forall i \in \mathbb{N}_{\leq a}. \quad (15)$$

PROOF. Given that the length of each interval \mathcal{U}_i is L_i (cf. (13)), the length of each sub-interval, obtained by uniformly dividing \mathcal{U}_i at the N_i samples, is $\frac{L_i}{N_i-1}$. Considering the Lipschitz continuity in (12), the rounding error for $\tilde{\mathcal{N}}_i(u)$ is bounded as follows

$$\|\tilde{\mathcal{N}}_i(u) - \mathcal{N}_i(u)\| \leq \frac{L_i}{N_i-1} \lambda_i. \quad (16)$$

If (15) hold for all $i \in \mathbb{N}_{\leq a}$, the following inequalities also hold

$$\frac{L_i}{N_i-1} \lambda_i \leq \epsilon. \quad (17)$$

Therefore, from (16) and (17), $\|\tilde{\mathcal{N}}_i(u) - \mathcal{N}_i(u)\| \leq \epsilon$ for all $i \in \mathbb{N}_{\leq a}$, and consequently (14) holds. \square

Based on Theorem 3.1, the number of samples used in the discretization of nonlinear activation functions, such as the $\mathcal{N}_{\text{TanH}}$ and $\mathcal{N}_{\text{Sigm}}$, described respectively in Eqs. (3) and (4), can be computed to ensure some desired accuracy. Without loss of generality, the approximation $\tilde{\mathcal{N}}_i(u)$ can be defined as follows:

$$\tilde{\mathcal{N}}_i(u) = \mathcal{N}_i(\mathcal{A}_i(u)), \quad (18)$$

where $\mathcal{A}_i : \mathcal{U}_i \mapsto \tilde{\mathcal{U}}_i$ is an arbitrary approximation operator, e.g. rounding and quantization.

For instance, consider that we want to obtain the function $\mathcal{N}_{\text{Sigm}}$, which approximates $\mathcal{N}_{\text{Sigm}}$ based on a discrete domain $\tilde{\mathcal{U}}$, with target accuracy $\epsilon = 0.01$. It is clear that $\mathcal{N}_{\text{Sigm}}$ is globally Lipschitz continuous with constant $\lambda_{\text{Sigm}} = 0.25$ since the $\sup_{u \in \mathbb{U}} |\mathcal{N}_{\text{Sigm}}(u)| = 0.25$, and $\mathcal{U} = \mathbb{R}$. Moreover, let us choose the following three intervals to define the approximation $\tilde{\mathcal{N}}_{\text{Sigm}}(u)$:

$$\mathcal{U}_1 = (-\infty, -20], \quad \mathcal{U}_2 = (-20, 20), \quad \mathcal{U}_3 = [20, \infty), \quad (19)$$

since the derivative of $\mathcal{N}_{\text{Sigm}}(u)$ is negligible for $u \in \mathcal{U}_1 \cup \mathcal{U}_3$, i.e. $\lambda_1 \approx 0$, and $\lambda_3 \approx 0$, while the constant λ_2 is equivalent to the global Lipschitz constant, i.e. $\lambda_2 = \lambda_{\text{Sigm}} = 0.25$. Now, we can use Eq. (15) to compute the number of samples in each interval necessary to ensure the desired accuracy $\epsilon = 0.01$. Accordingly, the numbers of samples are $N_1 = N_3 = 1$ and $N_2 = 1001$, since $L_2 = 40$ (cf. (13)). Notice that the approximators \mathcal{A}_i can be arbitrarily chosen. For this example, it is suggested to choose $\mathcal{A}_1 = -20$ and $\mathcal{A}_3 = 20$, because it is not necessary to have more samples than the limits of the intervals for \mathcal{U}_1 and \mathcal{U}_3 . Finally, \mathcal{A}_2 can be chosen as the half-towards-zero rounding with 3 decimal digits for floating-point and real ANNs, and as the underlying quantization function for fixed-point ANNs.

Fig. 5 illustrates the effect of the discretization when evaluating the sigmoid function. Notice that the approximation fits well for $\epsilon = 0.01$, and it becomes poor when ϵ increases.

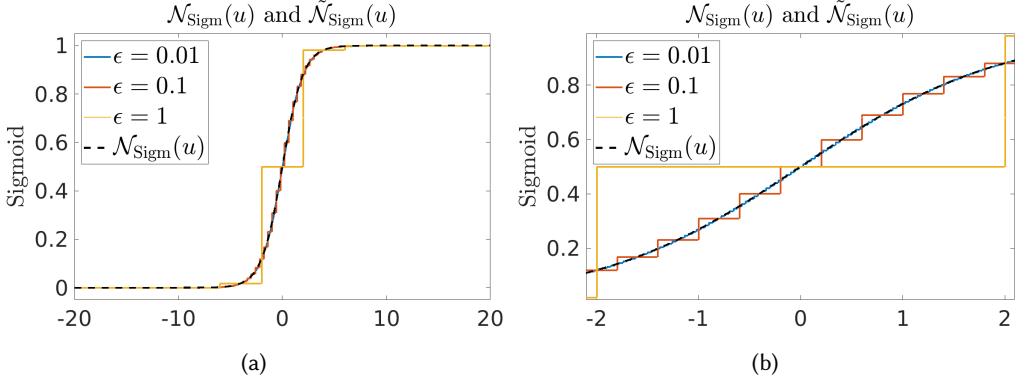


Fig. 5. Comparison between the real sigmoid N_{Sigm} and its discretizations \tilde{N}_{Sigm} for different values of ϵ : $\epsilon = 0.01$ ($N_2 = 1001$), $\epsilon = 0.1$ ($N_2 = 101$), $\epsilon = 1$ ($N_3 = 11$). Figure 5a depicts the sigmoid activation function and its approximations within the range $[-20, 20]$, and figure 5b zooms in to show the interval $[-2, 2]$.

3.4 Invariant inference via interval analysis

Converting the non-linear activation functions into lookup tables is an essential step towards efficient verification of ANN code. However, we can further improve our verification time by reducing the model checker search space. Indeed, given the sequential nature of the ANN computation, the small set \mathcal{H} of values allowed by the premise of the safety property (see Section 3.1) also constrains the range of the following intermediate computation steps. Thus, if we can explicitly derive these additional constraints on the intermediate variables, we can more succinctly tell the model checker where to look for counterexamples.

In general, deriving additional (overapproximated) constraints on intermediate computation steps falls under the umbrella of *invariant inference* [67]. For neural network code, which does not contain loops or dynamic memory allocation, we find that an interval invariant analysis suffices [58]. This method of invariant analysis computes lower and upper bounds on the value of each program variable (e.g., $a \leq x \leq b$, where a, b are constants and x is a variable), by propagating the initial set \mathcal{H} through the ANN with interval arithmetic rules. Note that more complex constraint propagation methods (zonotopes, polyhedra) exist in the literature [75], but whether the reduction in search space justifies the additional computational cost is an open problem.

On the more practical side, there are many tools to perform interval analysis of C code. In our experiments of Section 4 we use the Evolved Value Analysis (Eva) plugin of the open-source tool FRAMA-C. We then inject the intervals into the ANN code as additional pre-condition instructions `assume` on the intermediate variables. Finally, we compare this method with the native interval analysis support provided by the state-of-the-art verification tool ESBMC in Section 4.3.3 and find that combining them yields the best results.

3.5 Model checking of ANN implementations

Given the annotated C code from Sections 3.1 to 3.4, we are now tasked with answering the following verification question: do *all* inputs that satisfy the `assume` pre-conditions also satisfy the `assert` post-conditions? In other terms, can we find at least one specific input that violates the safety property? In this section we explain how to answer this question with state-of-the-art *model checking* techniques.

In general, model checking is concerned with verifying whether a given property ϕ holds for a finite state transition system $M(S, I, T)$ [16]. More formally, these mathematical objects are defined as follows:

- S is the set of states the system can be in;
- $I : S \rightarrow \{0, 1\}$ is an indicator function for the initial states;
- $T : S \rightarrow S$ is a transition function describing the system evolution;
- $\phi : S \rightarrow \{0, 1\}$ is an indicator function for the safe states.

In our case, the annotated ANN code defines these objects implicitly: S are all possible assignments of values to the variables in the program, I are all assignments that satisfy the assume pre-conditions, T is the semantic of each instruction in the code and ϕ are all assignments that satisfy the assert post-condition.

In practice, several state-of-the-art model checkers accept C code as input [10, 28, 29, 52]. Frequently, the input code is readily converted to static single assignment (SSA) form before further processing [19]. This has the advantage of making the underlying finite-state transition system more explicit. We show an example of such conversion in Figures 6a and 6b.

Note that in all our experiments of Section 4 we use ESBMC for this model checking step [28, 29]. Like any other state-of-the-art model checkers, ESBMC has been heavily optimized to reduce the verification time. However, not all of these optimization techniques apply to neural network code, which does not contain loops and other complex control flow structures. We clarify which techniques do apply to ANN code in the following Sections 3.6 and 3.7.

3.6 Incremental verification

The SMTLIB logic format introduced an assertion stack concept and the ability to push and pop assertions and off it [5]. In particular, some SMTLIB compliant SMT solvers have an internal stack of assertions, which we can add new assertions or remove old ones from this stack. The main idea here is to enable assertion retraction and lemma learning incrementally. The former allows one to add assertions to the formula, evaluate the result, then return the formula to its original form. The latter is when the SMT solver stores facts (in the form of lemmas over the formula variables). It has determined the formula, which may prove helpful in future checks of the formula.

Here, we enable the solver to use lemmas determined during previous checks for future checks, thereby optimizing the search procedure and potentially eliminating a large amount of formula state space to be searched. So we apply incremental SMT to verify neural net implementations, where the formula is built up in stages, and lemmas learned about the formula along the way.

This incremental verification is beneficial to exploring neural net implementations by ESBMC since they contain various *ite* operators (e.g. to represent ReLU activation functions). The existing operation of the SMT solver follows directly from ESBMC as follows. Once we produce an SSA program by symbolic execution from the neural net implementation, that program is converted to a fragment of first-order logic and translated to a form acceptable to the solver; after checking the formula satisfiability, the entire formula is discarded. Here, many *ite* operations will be converted, solved, and discarded during the neural net verification. Using *ite* retraction to build and deconstruct the formula could reduce SMT-conversion overhead, and lemma learning could lead to swifter verification times. The default SMT solver in ESBMC, Z3, claims lemma learning as a feature [21], thereby allowing us to evaluate its impact for verifying neural net implementations.

To use incremental SMT during neural net verification, we must identify ways to reuse the SMT formula by pushing and popping *ite* operations into the solver. In particular, we retain the formula produced for an *ite* operator, identify the common prefix between it and the next *ite* operator produced, and retract all the *ite* operations that can be evaluated. Then, we place the *ite* operators,

which could not be evaluated, on top of the remaining formula. Figure 6 illustrates this approach. Here, we have three *ite* operators located in lines 7, 9, and 11. During the symbolic execution, we check the guard’s satisfiability of the guard “ $a < 0$ ” in line 7 and concluded that it could either be evaluated as “true” or “false” since “ a ” can assume the values -3 and 2 . As a result, we cannot simplify this expression before checking the safety property in line 12. After that, we check the satisfiability of the guard “ $b < 0$ ” in line 9 and concluded that it evaluates to “false” since “ b ” can assume only positive numbers (0 and 5). So, we are thus able to simplify this expression. Lastly, we check the satisfiability of the guard “ $f < 0$ ” in line 11 and also conclude that it evaluates to “false” since “ f ” can assume only positive values (0 or 4).

(a)
(b)

(c)

```

1 int main() {
2     _Bool x, y;
3     int a, b, f;
4     x = nondet_bool();
5     y = nondet_bool();
6     a = ((2*x) - (3*y));
7     a = a < 0 ? 0 : a;
8     b = (x + (4*y));
9     b = b < 0 ? 0 : b;
10    f = ((3*x) + y);
11    f = f < 0 ? 0 : f;
12    assert(a <= 2 && b <= 5 && f <= 4);
13    return 0;
14 }
```

```

1 x1 == nondet_symbol(nondet0)
2 y1 == nondet_symbol(nondet1)
3 a1 == 2 * (int)x1 - 3 * (int)y1
4 a2 == (a1 < 0 ? 0 : a1)
5 b1 == (int)x1 + 4 * (int)y1
6 b2 == (b1 < 0 ? 0 : b1)
7 f1 == 3 * (int)x1 + (int)y1
8 f2 == (f1 < 0 ? 0 : f1)
9 (assert) a2 <= 2
10 (assert) b2 <= 5
11 (assert) f2 <= 4
```

```

1 x1 == nondet_symbol(nondet0)
2 y1 == nondet_symbol(nondet1)
3 a1 == 2 * (int)x1 - 3 * (int)y1
4 a2 == (a1 < 0 ? 0 : a1)
5 b1 == (int)x1 + 4 * (int)y1
6 f1 == 3 * (int)x1 + (int)y1
7 (assert) a2 <= 2
8 (assert) b1 <= 5
9 (assert) f1 <= 4
```

Fig. 6. (a) A simple neural net implemented in C. (b) The C program of (a) converted into SSA form. (c) A simplified version of the C program in (a).

3.7 Constant folding and slicing for search-space reduction

Our employed verification engine implements code optimizations when converting the neural net implementation to SMT, including *constant folding* and *slicing* [17]. Constant folding evaluates constants, including nondeterministic symbols, and propagates them throughout the resulting formula during encoding. In particular, we exploit the constant propagation technique to reduce the number of expressions associated with a particular neuron computation and activation function. Thus, we simplify the SSA representation using local and recursive transformations to remove functionally redundant expressions (for neuron computation and activation function) and redundant literals (for safety properties) as follows:

$$\begin{array}{ll}
 a \wedge \text{true} = a & a \wedge \text{false} = \text{false} \\
 a \vee \text{false} = a & a \vee \text{true} = \text{true} \\
 a \oplus \text{false} = a & a \oplus \text{true} = \neg a \\
 \text{ite}(\text{true}, a, b) = a & \text{ite}(\text{false}, a, b) = b \\
 \text{ite}(f, a, a) = a & \text{ite}(f, f \wedge a, b) = \text{ite}(f, a, b)
 \end{array}$$

We apply these simplifications to reduce the size of the formula and consequently achieve simplification within each time step and across time steps during the encoding of the neural net implementation. In Figure 6(c), we illustrated how to remove the activation function for the neuron b and output f via constant propagation.

Slicing removes expressions that do not contribute to checking a given safety property. For example, consider the code in Figure 6(a). If we are interested in checking the neural net’s output only, we could rewrite the assert statement in line 12 as $f \leq 4$. The resulting SSA would be sliced as follows:

```
x1 == nondet_symbol(nondet0) ∧ y1 == nondet_symbol(nondet1) ∧
f1 == 3 * (int)x1 + (int)y1 ∧ f2 == (f1 < 0 ? 0 : f1) ∧ f2 ≤ 4
```

In our experimental evaluation of Section 4.3.3, we have observed that *constant folding* and *slicing* can significantly reduce SMT solving time.

3.8 Illustrative example: robustness to adversarial images

We conclude this section with an illustrative example of our verification methodology. We do so in order to clarify the user side of the workflow illustrated in Figure 3. Finally, we report more details on the range of ANNs and safety properties that can be verified with our methodology, as well as the efficiency of doing so, in Section 4.

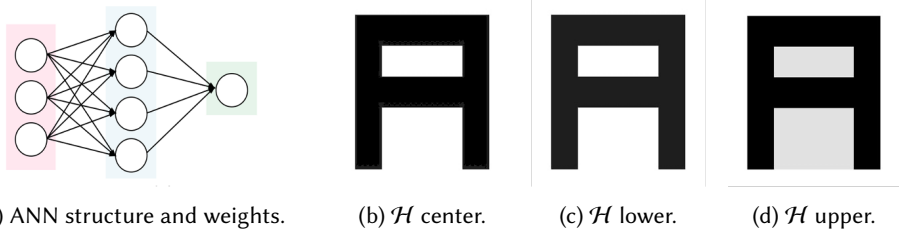


Fig. 7. Inputs of our verification approach: ANN implementation and safety property. In this example, we show the center, upper and lower extremes of the input region. Note that the lower extreme is in a lighter shade of gray than the center.

The present example shows how to verify a character recognition ANN. First, given the network architecture and weights in a high-level representation as in Figure 7a, convert them into C code. This task can be achieved through the popular machine learning libraries PyTorch [64], and Tensorflow [1] or, like in many of our experiments in Section 4, by converting from the mid-level representation NNet¹.

Second, encode the safety property by adding the corresponding pair of *assume* and *assert* instructions. In the present example we check for robustness around a specific input image, which we show in Figure 7b. More formally, we define the input region of our safety property (premise) as a set $\mathcal{H} = \{x : |x - x^d|_\infty \leq c\}$, where the centre point x^d corresponds to the 5×5 pixel values in the image of the character “A” in Figure 7b, and $c = 30$. For reference, we report the lower and upper bounds of \mathcal{H} in the gray image pixel domain in Figures 7c and 7d.

Likewise, we set the output region of the safety property (conclusion) as the set of all outputs that assign a higher score $y_A > y_k, \forall k \neq A$ to class “A” than to any other output classes. Note that

¹github.com/sisl/NNet

the final softmax layer typically included in classification ANNs can be omitted for robustness verification purposes as it is a monotonic function of the log-score of each class.

Third, the piece of C code undergoes a further sequence of transformations. On the one hand, we replace all floating-point arithmetic operations with the corresponding fixed point operational models if the input ANN is quantized. On the other hand, we replace any sigmoid, hyperbolic tangent, or otherwise non-piecewise-linear activation function with its corresponding discretized lookup table. After this, a static analysis tool like FRAMA-C propagates the input region \mathcal{H} through the ANN and annotates the code with additional `assume` instructions, representing the reachable interval of values of each intermediate variable.

Fourth, the annotated C code goes through a model checker that tries to falsify the safety property. In our experiments (see Section 4), we use ESBMC to do so, as it is a good representative of state-of-the-art SMT model checkers. If the model checker cannot verify the safety property, it will return a counterexample that falsifies it. Such counterexample represents a potential adversarial attack on the neural network. We show a few instances of adversarial attacks on our character recognition ANN in Figures 10, 11 and 12.

4 EXPERIMENTAL EVALUATION

In this section, we test the performance of the verification approach we introduced in Section 3. In this regard, we are mainly interested in two research questions. First, we want to establish the role of each of the optimization techniques introduced in Section 3 in reducing the total verification time. Since these techniques were first introduced for software verification in general, we are interested in finding their optimal configuration to verify ANNs in particular. Second, we want to understand how much the choice of quantization influences the verification process. Namely, if we were to verify the same property for different quantization levels, would we observe any difference in verification time or outcome?

We present our answers to these questions in the following way. In Section 4.1, we describe the datasets and ANNs that constitute our verification benchmarks. In Section 4.2, we formalize the experimental objectives that we are aiming to accomplish. In Section 4.3, we isolate the contribution of each component of our verification approach and propose the configuration that yields the best results performance-wise. Finally, in Section 4.4, we compare the performance and output of our verification approach across different quantization levels of the same problem. All benchmarks, tools, and results associated with the current evaluation are available for downloading at <https://tinyurl.com/y6xvze65>.

4.1 Description of the benchmarks

In our evaluation, we consider ANNs trained on two datasets: the UCI Iris dataset [24] and a vocalic character recognition dataset [69]. This section gives the details of the datasets themselves, the neural networks we trained on top of them, and the safety properties that we used to test our verification approach and our general experimental setup.

4.1.1 Iris benchmark. The Iris data set [24] consists of 50 samples from each of three species of Iris (Iris setosa, Iris virginica and Iris versicolor). The dataset contains both the length and width of the sepals and petals in centimeters (our inputs) and the iris specie label (our output). Here, we use TensorFlow version 1.4 [1] and keras [36] to train a feedforward neural network with layers of $4 \times 7 \times 3$ neurons, hyperbolic tangent activation functions, and softmax output layer. We train such a neural network to predict the correct Iris species with the backpropagation algorithm and cross-validation [11]. In terms of safety properties, we specify hyperrectangular input regions for each species: *setosa*, *versicolor*, and *virginica*. The center of these regions was

identified from the dataset with the granular fuzzy clustering algorithm in [18]. Then, for each of the four input variables, we computed its maximum range. With it, we generated nine regions R_s for each class, sharing the same center but with different sizes $s \in \{1, 2, 5, 8, 10, 20, 30, 40, 50\}$ of the hyperrectangle surrounding it, where s is a percentage representing the fraction of the maximum input range.

4.1.2 Vocalic benchmark. The vocalic dataset [69] consists of 200 gray-scale images with dimensions 5×5 pixels. Half of the dataset is composed of noisy versions of the base images illustrated in Fig. 8. The other half is composed of non-vocalic images. With it, we trained a feedforward neural network with architecture $25 \times 10 \times 4 \times 5$ and sigmoid activation functions. As Fig. 8 there are five output classes that the network learns to discriminate via backpropagation algorithm and cross-validation. As far as the safety properties are concerned, we specify five hypercubic input regions corresponding to the vocalic labels. The centers are defined by the base images in Fig. 8. Similarly to the Iris benchmark, we generate five instances L_s of these regions with different sizes $s \in \{10, 20, 40, 80, 120\}$, where s represents the hypercube side length.



Fig. 8. Vocalic images in benchmarks.

4.1.3 Experimental setup. We have conducted the experimental evaluation on a Intel(R) Xeon(R) CPU E5-2620 v4 @ 2.10GHz with 128 GB of RAM and Linux OS. All presented execution times are CPU times, *i.e.*, only the elapsed periods spent in the allocated CPUs, which was measured with the *times* system call [57]. All experimental results reported here were obtained by executing ESBMC v6.6.0² with a pre-defined prompt command,³ unless specifically noted, which is wrapped in a shell script to unwind a program iteratively. We set the execution timeout limit at 2 hours and the memory usage limit at 64GB for each benchmark.

4.2 Objectives

Our experimental evaluation has the following goals:

EG1 - Ablation study - Compare the performance of our verification approach under different parameters to identify the optimal configuration, and shed some light on the importance of each optimization technique presented in Section 3.

EG2 - Quantization effects - Evaluate the impact of different quantization granularities on the performance of our verification approach, and the quality of the adversarial examples it produces.

We cover them in Sections 4.3 and 4.4 respectively.

4.3 Ablation study

This section aims at evaluating the impact of different aspects of our approach on the total verification time. Here, our aim is both to discover the best configuration for our verification tool and shed some light on the importance of each technique for reducing the search space of the verification

²Available at <http://esbmc.org/>

³esbmc <file.c> -I <path-to-OM> -force-malloc-success -no-div-by-zero-check -no-pointer-check -no-bounds-check -incremental-bmc -interval-analysis -fixedbv

problem. Specifically, we address three choices in our verification approach: the choice of SMT solver, the choice of an interval analysis technique and the choice of parameters for the ESBMC verification engine.

4.3.1 SMT solvers comparison. As mentioned in Section 3, our approach relies on model checking to reason about the satisfiability of a given safety property concerning the ANN implementation. For the experiments of the present section, we have chosen ESBMC as our verification engine since it has been extensively evaluated at various SV-Comp [9] competitions, where it has consistently achieved state-of-the-art results [28]. More in detail, the ESBMC model checker takes care of converting the input C code into SMT formulae and then calls an external SMT solver. Currently, ESBMC supports three solvers: Boolector, Yices, and Z3. In general, they yield different verification results, both in terms of the generated counterexample (if any) and the verification time.

Here, we are interested in comparing the performance of such solvers in verifying ANN implementations. To this end, we run them on a subset of our benchmarks, i.e., Vocalic A with its L_s variations and a fixed-point representation of the corresponding ANN with word length $\langle 3, 4 \rangle$. While this choice is arbitrary, we believe it is representative of the computational characteristics of our benchmarks.

With that in mind, we summarize the results in Fig. 9, where we plot the verification time of each solver against the size s of the input region. Bear in mind that L_s represents the amount of non-determinism in the source code, i.e., the set of possible values that program constraints can assume in the state space search. Thus, as the size of the L_s region grows, so does the state space search, leading to more complex formulae to be solved.

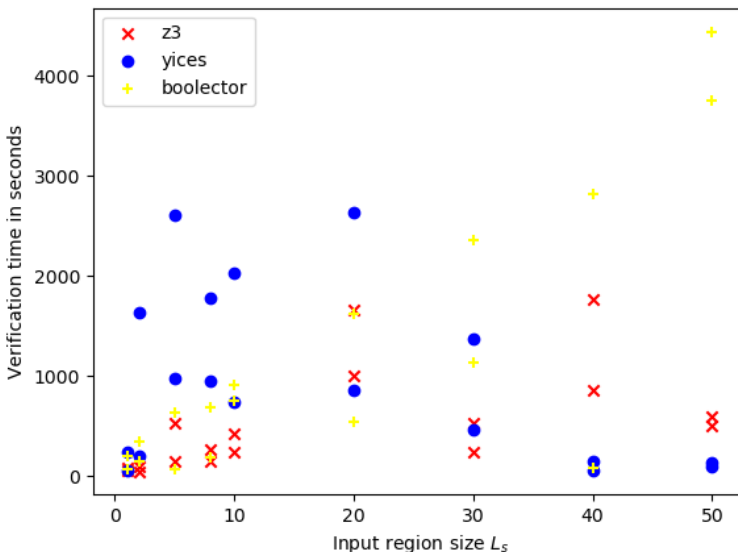


Fig. 9. Verification time of Boolector, Yices, and Z3 for input regions of increasing size.

As Fig. 9 shows, Z3 and Boolector are faster than Yices for small input regions, whereas for large input regions, the opposite is true. This is because the encoding of our ANN verification problem into SMT formulae is done with the formalism of *QF_AUFBV* logic. Here, *QF* stands for

quantifier-free formulas, A stands for the theory of arrays, UF stands for uninterpreted functions, and BV stands for the theory of fixed-sized bit-vectors. For this type of formulae, Yices represents the state-of-the-art SMT solver.⁴ Therefore, we explicitly specify Yices as our SMT solver for the upcoming experiments instead of Z3 or Boolector (the current default choice for ESBMC).

4.3.2 Interval analysis comparison. In Section 3 we introduced interval analysis as an essential pre-processing stage before running the verification engine on the ANN code. Here, we show the effect of disabling such an important step on the total verification time. Furthermore, we compare two approaches to interval analysis: the first requires FRAMA-C to annotate the ANN code with additional `assume` instruction. In contrast, the second requires running the ESBMC verification tool with an extra `interval-analysis` option enabled. Note that both of them compute hyperrectangular constraints over the program variables.

Our first experiment compares these two interval analysis tools on the vocalic dataset. We test only a few safety properties for simplicity, and we set the fixed-point quantization to $\langle 3, 4 \rangle$. The results are summarized in Table 1. Note how FRAMA-C has the largest impact on the verification time, but running both tools simultaneously gives us the best result. For this reason, we elect to run all of our remaining experiments with both tools enabled unless otherwise specified.

		ESBMC	
		Yes	No
FRAMA-C	Yes	36.6	38.8
	No	104.1	110.1

(a) Vocalic A, region size L_{10} .

		ESBMC	
		Yes	No
FRAMA-C	Yes	909.2	993.7
	No	1162.0	1111.3

(b) Vocalic A, region size L_{40} .

Table 1. Impact of FRAMA-C and native ESBMC interval analysis on the verification time (in seconds) of two safety properties from the vocalic benchmark with quantization $\langle 3, 4 \rangle$.

Our second experiment studies the impact of interval analysis on the verification of floating-point ANNs. To this end, we run our verification approach with and without the FRAMA-C pre-processing step, but we always enable the ESBMC native `interval-analysis` option. We verify all safety properties of the Iris and Vocalic datasets for completeness and report both verification time and verification outcome. The results in Table 2 are organized as follows: Safety Prop. is the specific safety property that we are verifying, Time is the verification time in seconds, Res is the verification outcome. The latter can signal that an adversarial case was found (F), no adversarial cases were found (NF), or we exhausted all time and/or memory resources before concluding (TO).

As Table 2 shows, interval analysis is better on average, even though it does increase the verification time in a small minority of cases. For the 27 benchmarks in the Iris dataset, interval analysis takes 10997 seconds to verify all benchmarks, whereas non-interval takes 19774 seconds to verify 24 benchmarks (3 exhausted the time limit). Similarly, for the 25 benchmarks in the vocalic dataset, interval analysis takes 17092 seconds to verify 21 benchmarks (4 exhausted the time limit). In contrast, non-interval takes 20094 seconds to verify 19 benchmarks (6 exhausted the time limit). Thus, interval analysis can verify more benchmarks in less time than the non-interval approach. At the same time, if we restrict our analysis on the subset of benchmarks that both approaches managed to solve, using interval analysis leads to a time reduction of 54% for the Iris benchmarks and 69% for the Vocalic benchmarks.

More specifically, interval analysis significantly reduces the verification time for Iris benchmarks, but it produces fewer counterexamples than having it disabled. At the same time, such a reduction

⁴<https://smt-comp.github.io/2020/results/qf-aufbv-single-query>

Iris		FRAMA-C			
		Yes		No	
Safety Prop.		Time	Res	Time	Res
Setosa	R_1	12.6	NF	-	NF
	R_2	10.8	NF	-	NF
	R_5	12.1	NF	895.2	NF
	R_8	14.4	NF	-	NF
	R_{10}	261.3	NF	1675.2	NF
	R_{20}	78.3	NF	2483.4	NF
	R_{30}	282.3	NF	1295.4	F
	R_{40}	190.2	F	135.6	F
	R_{50}	54.4	F	128.3	F
	R_1	9.0	NF	279.9	NF
Versicolor	R_2	61.3	NF	2779.8	NF
	R_5	148.9	NF	4711.2	NF
	R_8	230.2	NF	827.3	F
	R_{10}	305.5	NF	-	F
	R_{20}	782.3	NF	19.7	F
	R_{30}	1262.0	NF	20.3	F
	R_{40}	1591.6	NF	20.4	F
	R_{50}	1044.5	F	44.8	F
	R_1	10.1	NF	310.9	NF
	R_2	10.1	NF	1914.6	NF
Virginica	R_5	300.6	NF	1539.7	NF
	R_8	358.8	NF	414.7	F
	R_{10}	628.5	NF	165.3	F
	R_{20}	658.6	NF	23.4	F
	R_{30}	811.1	NF	26.2	F
	R_{40}	948.0	NF	33.3	F
	R_{50}	919.2	F	29.2	F

(a)

Vocalic		FRAMA-C			
		Yes		No	
Safety Prop.		Time	Res	Time	Res
“A”	L_{10}	7.3	NF	3773.3	F
	L_{20}	177.2	NF	-	TO
	L_{40}	2652.9	F	4105.6	F
	L_{80}	1915.6	F	671.5	F
	L_{120}	1358.2	F	133.2	F
“E”	L_{10}	2962.9	F	-	TO
	L_{20}	377.9	F	661.6	F
	L_{40}	178.0	F	669.4	F
	L_{80}	456.8	F	235.1	F
	L_{120}	142.0	F	182.6	F
“I”	L_{10}	917.3	F	852.3	F
	L_{20}	230.0	F	820.6	F
	L_{40}	151.4	F	317.2	F
	L_{80}	163.8	F	232.0	F
	L_{120}	173.1	F	325.7	F
“O”	L_{10}	-	TO	-	TO
	L_{20}	3337.4	F	5426.4	F
	L_{40}	-	F	254.0	F
	L_{80}	83.2	F	398.7	F
	L_{120}	156.2	F	306.4	F
“U”	L_{10}	166.0	NF	-	TO
	L_{20}	-	TO	-	TO
	L_{40}	-	TO	-	TO
	L_{80}	398.2	F	441.8	F
	L_{120}	1086.5	F	286.9	F

(b)

Table 2. Impact of FRAMA-C interval analysis on the verification time (in seconds) of all safety properties from the Iris (a) and Vocalic (b) benchmarks in floating-point representation. The verification outcome is reported as falsified (F), not falsified (NF) or timeout(TO).

in verification time can be crucial for avoiding timeouts. Even though our ANN for the Iris dataset is relatively small, disabling interval analysis leads to timeout in 15% of cases. In contrast, the neural network for the Vocalic dataset is larger, with a $25 \times 10 \times 4 \times 5$ architecture instead of just $4 \times 7 \times 3$. As a consequence, verifying the safety properties is computationally more challenging and timeouts happened more frequently. However, even on this more challenging benchmark, interval analysis can significantly improve the verification efficiency.

Note that we observed similar performance improvement in our previous experiments over a large set of open-source benchmarks when enabling invariant generation [28]. In particular, in the study above, invariant generation based on intervals allowed us to verify 7% more programs using a k -induction proof rule. Therefore, we chose to enable the interval-analysis option in ESBMC for the upcoming experiments explicitly.

4.3.3 ESBMC parameters comparison. When it comes to evaluating the performance of ESBMC, there is one additional experiment to be carried out. In particular, as an award-winning verification tool, ESBMC provides various parameters to handle different scenarios, allowing the user to customize how ESBMC tackles the verification task.

After a careful review of ESBMC’s documentation, we have chosen to evaluate the combination of the following parameters, as they are crucial in the verification of ANNs:

- **interval-analysis.** Enables native interval analysis, as detailed in Section 4.3.2.
- **no-propagation.** Disables the propagation of constants used to generate a minimal set of SSAs in the symbolic engine.
- **no-simplify.** Disables the simplification of expressions, effectively neutering constant propagation so that no fact is statically determined to be true or false, and always end up exploring to the top of the unwind bound.
- **no-slicing.** Disable slicing step. Slicing [20] is a mechanism for eliminating redundant or irrelevant portions of a program. In ESBMC, this is applied to the SSA program before it is encoded to SMT to reduce the number of variable assignments by identifying variables not used to evaluate any property assertion.

From our prior experience of participating in software verification and testing competitions (e.g., SV-COMP and Test-Comp), these flags play an essential role in tuning ESBMC to checking the given set of benchmarks [28, 31, 59]. Here, we evaluate the performance of different parameters on a small subset of our NN benchmarks, *i.e.*, the L_{10} and L_{40} safety properties of the Vocalic dataset, both with and without FRAMA-C interval analysis. For the sake of simplicity, we also set the fixed-point representation to $\langle 3, 4 \rangle$. The results are summarized in Table 3, where we start with our best configuration (interval-analysis) and then add each flag incrementally to the command-line parameters of ESBMC.

	FRAMA-C	
	Yes	No
interval-analysis	36.6	104.1
no-propagation	36.5	111.5
no-simplify	1614.6	3584.6
no-slicing	4517.0	4544.2

(a) Vocalic A, region size L_{10} .

	FRAMA-C	
	Yes	No
interval-analysis	909.2	1162.0
no-propagation	909.2	1156.8
no-simplify	3429.5	1262.0
no-slicing	4459.8	4571.9

(b) Vocalic A, region size L_{40} .

Table 3. Effect of the main options of ESBMC on the verification time in conjunction with FRAMA-C interval analysis. Note that each option is added on top of all the preceding ones. The two vocalic benchmarks were tested with quantization $\langle 3, 4 \rangle$.

As one can see, adding the no-propagation flag has an almost negligible effect on the verification time. In contrast, no-simplify and no-slicing degrade the performance significantly. This shows that constant propagation, a useful technique for general software verification, has less of an impact when checking robustness properties for ANN implementations. In contrast, expression simplification and slicing retain their crucial role in reducing the search space.

These results successfully answer **EG1 - Ablation study**: we identified an optimal configuration for the ESBMC verification engine, which consists of using the SMT solver Yices and the interval-analysis option. Moreover, we quantified the importance of interval analysis, constant propagation, expression simplification and slicing on the verification time.

4.4 Verification of fixed- and floating-point ANNs

In Section 4.3 we established what the best configuration of our verification method is by comparing its runtime under different scenarios. Similarly, in the present section, we compare its verification time and output along another dimension: the quantization level of the ANN. In this regard, we have two results. The first is quantitative and correlates the verification time with the granularity of the ANN quantization. The second is qualitative and shows that different quantization levels may yield opposite verification outcomes for the same safety property.

4.4.1 Effects of quantization on verification time. First, let us comment on how the quantization of an ANN affects the verification time of its safety properties. In this regard, we run an empirical comparison between different quantization levels: a detailed description of our results can be found in Tables 4 and 5. Safety Prop. is the specific safety property that we are verifying, Time is the verification time in seconds, Res is the verification outcome. Additionally, in the latter column, NF shows that no adversarial case was found. F shows that an adversarial case was found. TO shows that exhaustion of resources (memory and/or time) occurred. Finally, the $\langle k, l \rangle$ notation refers to the integer part of the fixed word length k and its fractional part l .

Iris		Float 32-bit		Fixed <3,4>		Fixed <7,8>		Fixed <15,16>	
Safety Prop.		Time	Res	Time	Res	Time	Res	Time	Res
Setosa	R_{10}	261.281	NF	133.704	F	124.951	F	1241.478	F
	R_{20}	78.285	NF	141.849	F	126.955	F	1519.171	F
	R_{30}	282.274	NF	134.286	F	124.065	F	902.818	F
	R_{40}	190.184	F	135.471	F	125.278	F	895.241	F
	R_{50}	54.445	F	138.241	F	124.400	F	831.362	F
Versicolor	R_{10}	305.529	F	140.496	F	122.102	F	1038.383	F
	R_{20}	782.294	F	146.130	F	121.217	F	1130.89	F
	R_{30}	1262.024	F	147.385	F	123.195	F	1114.291	F
	R_{40}	1591.633	F	148.617	F	122.247	F	1202.792	F
	R_{50}	1044.461	F	143.613	F	128.859	F	1325.709	F
Virginica	R_{10}	628.477	F	146.462	NF	120.725	NF	973.873	F
	R_{20}	658.576	F	147.162	NF	122.375	NF	986.941	F
	R_{30}	811.121	F	145.599	NF	121.852	NF	979.725	F
	R_{40}	948.028	F	142.958	NF	122.457	NF	834.663	F
	R_{50}	919.181	F	142.709	NF	126.962	NF	995.062	F

Table 4. Impact of ANN quantization on the verification time (in seconds) of the Iris safety properties. The verification outcome is reported as falsified (F), not falsified (NF) or timeout(TO).

As Tables 4 and 5 show, a key characteristic of our approach is that the verification time increases as the word length increases. For the Iris benchmarks using $\langle 3, 4 \rangle$ fixed-point representation, we have an average time of 142.31 seconds. Using a more granular $\langle 7, 8 \rangle$ representation, we have an

Vocalic		Float 32-bit		Fixed <3,4>		Fixed <7,8>		Fixed <15,16>	
Safety Prop.		Time	Res	Time	Res	Time	Res	Time	Res
“A”	L_{10}	7.318	NF	33.223	NF	34.208	NF	36.201	NF
	L_{20}	177.212	NF	32.100	NF	97.402	NF	80.364	NF
	L_{40}	2652.885	F	34.017	NF	771.893	F	46.002	NF
	L_{80}	1915.641	F	33.625	NF	814.494	F	35.023	F
	L_{120}	1358.232	F	33.189	NF	746.259	F	748.847	F
“E”	L_{10}	2962.855	F	31.575	NF	45.405	NF	979.920	NF
	L_{20}	377.853	F	32.365	NF	33.283	NF	33.202	NF
	L_{40}	178.012	F	33.354	NF	758.896	F	769.591	F
	L_{80}	456.809	F	719.692	F	758.352	F	884.615	TO
	L_{120}	141.973	F	704.243	F	729.220	F	665.928	TO
“I”	L_{10}	917.303	F	31.731	NF	45.405	NF	79.869	NF
	L_{20}	229.96	F	32.241	NF	699.564	F	851.093	F
	L_{40}	151.386	F	34.071	NF	739.997	F	866.673	F
	L_{80}	163.766	F	737.063	F	739.351	F	861.355	F
	L_{120}	173.097	F	738.303	F	729.588	F	1083.975	F
“O”	L_{10}	-	TO	36.514	NF	34.022	NF	40.809	NF
	L_{20}	3337.401	F	35.312	NF	734.379	F	829.075	F
	L_{40}	-	F	37.873	NF	725.426	F	843.272	F
	L_{80}	83.18	F	709.559	F	753.564	F	854.181	F
	L_{120}	156.249	F	701.559	F	780.250	F	912.291	F
“U”	L_{10}	165.991	NF	768.094	NF	33.344	NF	40.210	NF
	L_{20}	-	TO	753.971	NF	158.287	NF	204.746	NF
	L_{40}	-	TO	758.297	NF	720.630	F	1264.303	F
	L_{80}	398.23	F	766.470	F	774.463	F	1339.900	F
	L_{120}	1086.483	F	759.743	F	846.646	F	1496.300	F

Table 5. Impact of ANN quantization on the verification time (in seconds) of the Vocalic safety properties. The verification outcome is reported as falsified (F), not falsified (NF) or timeout(TO).

average time of 123.84 seconds. For the most precise $\langle 15, 16 \rangle$ representation, we had an average time of 1064.82 seconds. Similarly, for the Vocalic benchmark, the average verification time ranges from 343.52 seconds to 532.17 seconds and 633.90 seconds as the fixed-point word-length increases from $\langle 3, 4 \rangle$ to $\langle 7, 8 \rangle$ and $\langle 15, 16 \rangle$.

In contrast, when we analyze the floating-point representation results, the average verification time is 654.52 seconds for the Iris dataset and 813.90 seconds for the vocalic dataset. These results are in the same order of magnitude as those of the $\langle 15, 16 \rangle$ fixed-point representation. There two important factors that can explain such behavior: first, the floating-point representation in question uses 32 bits, the same word length of the $\langle 15, 16 \rangle$ representation; second, the ESBMC verification engine has been optimized for floating-point verification [30], a fact that could slightly bias the results against fixed-point ANNs in Tables 4 and 5.

This empirical result is especially interesting because it seems to run contrary to the theoretical conclusions in [39]. More specifically, the authors of [39] prove that the verification of quantized ANN belongs to a harder computational class than the verification of their real-valued counterparts. While practical verification techniques tend to exploit regularities that theoretical worst-case analysis cannot consider, it would be natural to think that verifying quantized ANNs is also harder

in practice. Instead, our experiments reveal a seemingly opposite trend. That is, the more granularity we allow in our fixed-point representation (thus bringing us closer to approximating real-valued arithmetic), the more our verification time *increases*. In conclusion, quantization appears to be a valuable technique for reducing the power consumption of ANNs and the verification time of their properties.

4.4.2 Effects of quantization on adversarial examples. Second, let us comment on the effect of ANN quantization on the counterexamples returned by our verification approach. As Tables 4 and 5 show, the verification outcome of the same safety property changes depending on the ANN representation we choose. This is because the different quantization granularities may either hide or reveal specific vulnerabilities in the ANN computation. At the same time, even if the verification outcome is the same, and the safety property is falsifiable (F), the counterexamples returned by the verification engine may be different.

Here, we present a qualitative comparison between these counterexamples, which are also known as *adversarial examples* in the context of machine learning research. Specifically, we focus on our three levels of fixed-point quantization, namely $\langle 3, 4 \rangle$, $\langle 7, 8 \rangle$ and $\langle 15, 16 \rangle$. For these, we present a selection of adversarial examples from the Vocalic benchmark in Figures 10, 11 and 12 respectively. Each figure contains pairs of images, where the center of the input region is on the left, and its corresponding adversarial example is on the right.

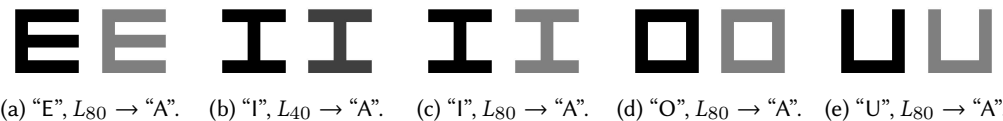


Fig. 10. Vocalic adversarial examples for the $\langle 3, 4 \rangle$ fixed-point representation.

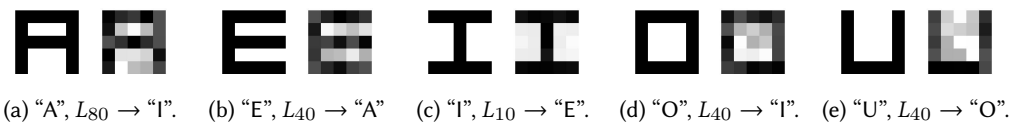


Fig. 11. Vocalic adversarial examples for the $\langle 7, 8 \rangle$ fixed-point representation.

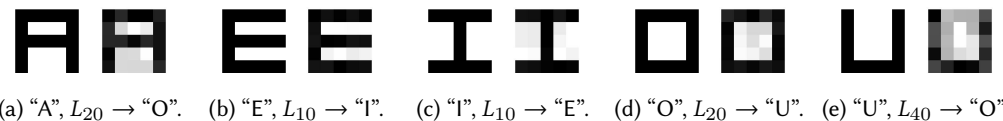


Fig. 12. Vocalic adversarial examples for the $\langle 15, 16 \rangle$ fixed-point representation.

As Figures 10, 11 and 12 show, the granularity of the ANN quantization has a significant effect on the quality of the adversarial examples. On the one hand, coarser fixed-point representations like $\langle 3, 4 \rangle$ restrict the search space to fewer gray-scale levels, which is clearly seen in Fig. 10. On the other hand, finer quantizations like $\langle 15, 16 \rangle$ let the verification engine produce counterexamples with minimal noise spread across the whole image (see Fig. 12). The latter behavior is typical of floating-point ANNs. It is especially dangerous for this specific case of image classification, as such adversarial examples may go undetected even by a human observer [73].

These results successfully answer **EG2 - Quantization effects**: we established that the verification time of our approach is positively correlated with the word length of the ANN quantization. Moreover, we showed that the type of adversarial noise changes depending on the quantization level.

4.5 Limitations

We believe the work we present in this paper is an important milestone towards the efficient verification of fixed- and floating-point ANNs with arbitrary activation functions. However, we still want to highlight a few limitations to our verification approach that need to be addressed in future work.

First, we handle non-linear activation functions by replacing them with lookup tables (see Section X). Even with a proper resolution, a lookup table will always be an approximation of the original function. Our experiments used lookup tables with a resolution of three decimal places and correctly validated all adversarial cases with MATLAB. However, we cannot exclude that our verification approach may produce incorrect adversarial examples in other ANN verification scenarios. This constitutes a potential threat to the validity of our method.

Second, the biggest challenge in ANN verification is scaling to large neural networks. In this regard, our Iris and Vocalic benchmarks are small to medium-sized. Furthermore, the dataset themselves are small, which probably generated ANNs with low robustness to adversarial attacks. Both of these factors contribute to keeping the dimensionality of the SMT formulae low and thus help our method achieve competitive verification times. A thorough comparison with other state-of-the-art methods is required.

5 RELATED WORK

This work's main contribution is providing a sound verification approach for checking the safety of MLPs with arbitrary activation functions and taking into account the FWL effects in the weights and bias due to fixed-point implementation. SMT-based approaches [43, 49, 50, 65, 69] have been used for safety verification of ANNs. The advantage of those techniques is the SMT solvers' soundness; however, there is an important drawback: the scalability is limited since they are sensitive to the ANN complexity. For this reason, most of them are not able to deal with large ANNs.

Wang *et al.* [78] propose an efficient approach for checking different safety properties of large neural networks, aiming at finding adversarial cases. Their approach is based on two main ideas. First, symbolic linear relaxation combines symbolic interval analysis and linear relaxation to create an efficient propagation method for tighter estimations. Second, directed-constraint refinement, which identifies nodes whose output is overestimated and iteratively refines their output ranges. Those two techniques are implemented in a tool called Neurify that was validated against multiple ANN architectures. Furthermore, to scale up their verification framework, they have implemented their code using multi-threaded programming techniques. However, as the previous tools [43, 49, 65], Neurify only supports ReLU activation functions. Katz *et al.* [50] present the Marabou that extends the Reluplex and uses lazy search to deal with the nonlinearities of activation functions, allowing to verify ANNs with any piecewise-linear activation functions.

Recently, set-theoretic methods for reachability-based verification have been proposed for verifying ANN-controlled closed-loop systems. In particular, Tran *et al.* propose the NNV tool [75], which over-approximates the exact reachable set by approximating the exact reachable set after applying an activation function. It allows supporting hyperbolic tangent and sigmoid activation functions. Other approaches [41, 46] also employ set-theoretic methods and polynomial approximations of

hyperbolic tangent and sigmoid, using Taylor’s [46] or Bernstein’s [41] polynomials. Our approach also allows verifying ANNs with non-linear activation functions by approximating them. The approximation is based on a lookup table to avoid non-linear operators’ use in the SMT solvers. This approach allows supporting any piecewise continuous activation function.

Robustness and explainability are the core properties of this study, and applying those properties to ANNs has shown impressive experimental results. Explainability showed a vital property to evaluate safety in ANNs: the core idea is to obtain an explanation for an adversarial case by observing the pattern activation behavior of a subset of neurons described by a given invariant. Gopinath *et al.* presented formal [33] and data-driven [34] techniques to extract properties from ANNs, which may be used as formal specifications for the ANNs. It is a crucial result to ensure the explainable adversarial examples.

Robustness is the ability to ensure safe outputs under the presence of disturbances and uncertainties, such as input noises and implementation issues [32]. In this sense, Dey *et al.* [23] provide a parametric regularization methodology to improve the robustness of ANNs concerning additive noises. However, the sensitivity to the FWL effects is not considered in that approach. The ANNs are designed to work in real arithmetic; however, it is already shown that safety violations may occur due to the floating-point [47] and fixed-point [32] implementations. In particular, Baranowski *et al.* presented a practical SMT-based approach for verifying neural networks’ properties considering fixed-point arithmetic. Their approach employs a realistic model of the FWL effects that includes different rounding and overflows models. However, as shown by Henziger *et al.* [39] the scalability of this kind of approach is compromised due to the hardness of verification of fixed-point implementations of ANNs. Therefore, a new method for verification of fixed-point implementations based on abstract interpretation is proposed in [39] to reduce the complexity and increase the scalability. However, that method can only verify ANNs with piecewise linear activation functions since it does not consider the propagation of FWL effects through generic non-linear functions. Our approach also considers the FWL effects of fixed-point implementations of ANNs based on an efficient FWL abstract model that reduces the complexity of verifying those ANNs. Our experiments and previous works on verification of fixed-point digital controllers [14] indicated that the scalability is not compromised by the use of this FWL abstract model.

Our approach implemented on top of ESBMC has some similarities with other techniques described here, e.g., regarding the covering methods proposed by Sun *et al.* [72], model checking to obtain adversarial cases proposed by Huang *et al.* [43], and incremental verification of ANNs implemented in CUDA by Sena *et al.* [69]. However, the main contribution concerns our requirements and how we handle, with invariant inference, the actual implementations of ANNs with non-linear activation functions, also considering FWL effects. Moreover, the latter results in promptly deployable ANNs, which could be integrated into a unified design framework. Only ANNs’ weights, bias descriptors, and desired input regarding a dataset are required to run our proposed safety verification. For tools such as DeepConcolic [72] and DLV [43], obtaining adversarial cases or safety guarantees in customized ANNs depends on the intrinsic characteristics of the models. For instance, in their implementations, they do not support complex non-linear activation functions. Moreover, Sena *et al.* [69] do not exploit invariant inference to prune the state space exploration, which is done in our proposed approach.

6 CONCLUSIONS

The verification of ANNs has recently attracted considerable attention, with notable approaches using optimization, reachability and satisfiability methods. While the former two come with the promise of scaling to large neural networks, they achieve such a goal by relaxing and approximating

the verification problem. In contrast, satisfiability methods are exact by construction but are confronted with the full complexity of the original verification problem.

In this paper, we propose a satisfiability modulo theory (SMT) approach to address the problem of ANN verification. More specifically, we view the ANN not as an abstract mathematical model but as a concrete piece of software, which performs a sequence of fixed- or floating-point arithmetical operations. We can borrow several techniques from software verification and seamlessly apply them to ANN verification with this view. In this regard, we center our verification framework around incremental model checking (IMC) and empirically show the importance of interval analysis, constant folding and slicing in reducing the total verification time. Furthermore, we propose a tailored discretization technique for non-linear activation functions that allow us to verify ANNs beyond the piecewise-linear assumptions that many state-of-the-art methods are restricted to.

Besides, in the course of our experimental evaluation, we uncovered an important relationship between the granularity of the ANN quantization and the verification time of its properties. The more granular the quantization, the larger the search space and thus the more prolonged the verification time. This is contrary to the main existing theoretical result in the literature, which states that verifying quantized ANNs computationally harder than verifying real-valued ones. However, further research is needed to shed more light on this phenomenon.

Finally, we believe that the problem of verifying ANNs is still open. More specifically, it is unclear which set of techniques yields the best performance when scaling to large networks. In this regard, our future work includes comparing our verification approach to other existing techniques and an effort to optimize our verification performance even further.

REFERENCES

- [1] Martín Abadi, Paul Barham, Jianmin Chen, Zhifeng Chen, Andy Davis, Jeffrey Dean, Matthieu Devin, Sanjay Ghemawat, Geoffrey Irving, Michael Isard, et al. 2016. Tensorflow: A system for large-scale machine learning. In *12th {USENIX} symposium on operating systems design and implementation ({OSDI} 16)*. 265–283.
- [2] Bowen Alpern and Fred B Schneider. 1987. Recognizing safety and liveness. *Distributed computing* 2, 3 (1987), 117–126.
- [3] Marek Baranowski, Shaobo He, Mathias Lechner, Thanh Son Nguyen, and Zvonimir Rakamarić. 2020. An SMT Theory of Fixed-Point Arithmetic. In *Automated Reasoning*, Nicolas Peltier and Viorica Sofronie-Stokkermans (Eds.). Springer International Publishing, Cham, 13–31.
- [4] Clark Barrett, Christopher L Conway, Morgan Deters, Liana Hadarean, Dejan Jovanović, Tim King, Andrew Reynolds, and Cesare Tinelli. 2011. Cvc4. In *International Conference on Computer Aided Verification*. Springer, 171–177.
- [5] Clark Barrett, Pascal Fontaine, and Cesare Tinelli. 2016. The Satisfiability Modulo Theories Library (SMT-LIB). www.SMT-LIB.org.
- [6] Clark Barrett, Aaron Stump, Cesare Tinelli, et al. 2010. The smt-lib standard: Version 2.0. In *Proceedings of the 8th international workshop on satisfiability modulo theories (Edinburgh, England)*, Vol. 13. 14.
- [7] Clark Barrett and Cesare Tinelli. 2018. Satisfiability modulo theories. In *Handbook of Model Checking*. Springer, 305–343.
- [8] Osbert Bastani, Yani Ioannou, Leonidas Lampropoulos, Dimitrios Vytiniotis, Aditya Nori, and Antonio Criminisi. 2016. Measuring Neural Net Robustness with Constraints. In *Advances in Neural Information Processing Systems*, D. Lee, M. Sugiyama, U. Luxburg, I. Guyon, and R. Garnett (Eds.), Vol. 29. Curran Associates, Inc. <https://proceedings.neurips.cc/paper/2016/file/980ecd059122ce2e50136bda65c25e07-Paper.pdf>
- [9] Dirk Beyer. 2021. Software verification: 10th comparative evaluation (SV-COMP 2021). *Tools and Algorithms for the Construction and Analysis of Systems* 12652 (2021), 401.
- [10] Dirk Beyer and M. Erkan Keremoglu. 2011. CPAchecker: A Tool for Configurable Software Verification. In *Computer Aided Verification*, Ganesh Gopalakrishnan and Shaz Qadeer (Eds.). Springer Berlin Heidelberg, Berlin, Heidelberg, 184–190.
- [11] Christopher Bishop. 2006. *Pattern Recognition and Machine Learning*. Springer.
- [12] Elena Botoeva, Panagiotis Kouvaros, Jan Kronqvist, Alessio Lomuscio, and Ruth Misener. 2020. Efficient Verification of ReLU-Based Neural Networks via Dependency Analysis. *Proceedings of the AAAI Conference on Artificial Intelligence* 34, 04 (April 2020), 3291–3299. <https://doi.org/10.1609/aaai.v34i04.5729>

- [13] Robert Brummayer and Armin Biere. 2009. Boolector: An efficient SMT solver for bit-vectors and arrays. In *International Conference on Tools and Algorithms for the Construction and Analysis of Systems*. Springer, 174–177.
- [14] Lennon C. Chaves, Hussama I. Ismail, Iury V. Bessa, Lucas C. Cordeiro, and Eddie B. de Lima Filho. 2019. Verifying fragility in digital systems with uncertainties using DSVerifier v2.0. *J Syst Softw* 153, 2019 (2019), 22–43.
- [15] Chih-Hong Cheng, Georg Nührenberg, Chung-Hao Huang, and Harald Ruess. 2018. Verification of Binarized Neural Networks via Inter-neuron Factoring. In *Verified Software. Theories, Tools, and Experiments*, Ruzica Piskac and Philipp Rümmer (Eds.). Springer International Publishing, Cham, 279–290.
- [16] Edmund M. Clarke, Thomas A. Henzinger, and Helmut Veith. 2018. *Introduction to Model Checking*. Springer International Publishing, Cham, 1–26. https://doi.org/10.1007/978-3-319-10575-8_1
- [17] Lucas C. Cordeiro. 2011. *SMT-based bounded model checking of multi-threaded software in embedded systems*. Ph.D. Dissertation. University of Southampton, UK. <http://eprints.soton.ac.uk/186011/>
- [18] Luiz Alberto Queiroz Cordovil, Pedro Henrique Silva Coutinho, Iury Valente de Bessa, Marcos Flávio Silveira Vasconcelos D’Angelo, and Reinaldo Martinez Palhares. 2020. Uncertain Data Modeling Based on Evolving Ellipsoidal Fuzzy Information Granules. *IEEE Transactions on Fuzzy Systems* 28, 10 (2020), 2427–2436. <https://doi.org/10.1109/TFUZZ.2019.2937052>
- [19] Ron Cytron, Jeanne Ferrante, Barry K. Rosen, Mark N. Wegman, and F. Kenneth Zadeck. 1991. Efficiently computing static single assignment form and the control dependence graph. *ACM TRANSACTIONS ON PROGRAMMING LANGUAGES AND SYSTEMS* 13 (1991), 451–490.
- [20] Andrea De Lucia. 2001. Program slicing: Methods and applications. In *Proceedings First IEEE International Workshop on Source Code Analysis and Manipulation*. IEEE, 142–149.
- [21] Leonardo De Moura and Nikolaj Bjørner. 2008. Z3: An efficient SMT solver. In *International conference on Tools and Algorithms for the Construction and Analysis of Systems*. Springer, 337–340.
- [22] Rodrigo de Salvo Braz, Ciaran O'Reilly, Vibhav Gogate, and Rina Dechter. 2016. Probabilistic Inference Modulo Theories. In *IJCAI*.
- [23] Prasenjit Dey, Kaustuv Nag, Tandra Pal, and Nikhil R. Pal. 2018. Regularizing Multilayer Perceptron for Robustness. *IEEE Transactions on Systems, Man, and Cybernetics: Systems* 48, 8 (Aug. 2018), 1255–1266. <https://doi.org/10.1109/tsmc.2017.2664143>
- [24] Dheeru Dua and Casey Graff. 2017. UCI Machine Learning Repository. <http://archive.ics.uci.edu/ml>
- [25] K Dvijotham, R Stanforth, S Gowal, T Mann, and P Kohli. 2018. A dual approach to scalable verification of deep networks. In *34th Conference on Uncertainty in Artificial Intelligence 2018, UAI 2018*, Vol. 2. 550–559.
- [26] Kevin Eykholt, Ivan Evtimov, Earlene Fernandes, Bo Li, Amir Rahmati, Chaowei Xiao, Atul Prakash, Tadayoshi Kohno, and Dawn Song. 2018. Robust Physical-World Attacks on Deep Learning Visual Classification. In *Conference on Computer Vision and Pattern Recognition*. 1625–1634.
- [27] Mahyar Fazlyab, Manfred Morari, and George J. Pappas. 2020. Safety Verification and Robustness Analysis of Neural Networks via Quadratic Constraints and Semidefinite Programming. *IEEE Trans. Automat. Control* (2020), 1–15. <https://doi.org/10.1109/tac.2020.3046193>
- [28] Mikhail Gadelha, Felipe Monteiro, Lucas Cordeiro, and Denis Nicole. 2019. ESBMC v6.0: Verifying C Programs Using k-Induction and Invariant Inference - (Competition Contribution). In *28th International Conference on Tools and Algorithms for the Construction and Analysis of Systems*. 209–213.
- [29] Mikhail Gadelha, Felipe Monteiro, Jeremy Morse, Lucas Cordeiro, Bernd Fischer, and Denis Nicole. 2018. ESBMC 5.0: an industrial-strength C model checker. In *33rd International Conference on Automated Software Engineering*. 888–891.
- [30] Mikhail Y. R. Gadelha, Lucas C. Cordeiro, and Denis A. Nicole. 2020. An Efficient Floating-Point Bit-Blasting API for Verifying C Programs. *CoRR* abs/2004.12699 (2020).
- [31] Mikhail Y. R. Gadelha, Rafael Menezes, Felipe R. Monteiro, Lucas C. Cordeiro, and Denis A. Nicole. 2020. ESBMC: Scalable and Precise Test Generation based on the Floating-Point Theory - (Competition Contribution). In *23rd International Conference Fundamental Approaches to Software Engineering (FASE) 2020 (LNCS, Vol. 12076)*. 525–529.
- [32] Mirco Giacobbe, Thomas A. Henzinger, and Mathias Lechner. 2020. How Many Bits Does it Take to Quantize Your Neural Network?. In *Tools and Algorithms for the Construction and Analysis of Systems*, Armin Biere and David Parker (Eds.). Springer International Publishing, Cham, 79–97.
- [33] Divya Gopinath, Hayes Converse, Corina Pasareanu, and Ankur Taly. 2019. Property Inference for Deep Neural Networks. In *2019 34th IEEE/ACM International Conference on Automated Software Engineering (ASE)*. IEEE. <https://doi.org/10.1109/ase.2019.00079>
- [34] Divya Gopinath, Guy Katz, Corina S. Păsăreanu, and Clark Barrett. 2018. DeepSafe: A Data-Driven Approach for Assessing Robustness of Neural Networks. In *Automated Technology for Verification and Analysis*. Springer International Publishing, 3–19. https://doi.org/10.1007/978-3-030-01090-4_1

[35] Alex Graves. 2012. *Supervised Sequence Labelling with Recurrent Neural Networks*. Springer, Berlin. <https://doi.org/10.1007/978-3-642-24797-2>

[36] Antonio Gulli and Sujit Pal. 2017. *Deep learning with Keras*. Packt Publishing Ltd.

[37] Yunhui Guo. 2018. A Survey on Methods and Theories of Quantized Neural Networks. *CoRR* abs/1808.04752 (2018). arXiv:1808.04752 <http://arxiv.org/abs/1808.04752>

[38] Dan Hendrycks and Kevin Gimpel. 2020. Gaussian Error Linear Units (GELUs). arXiv:1606.08415 [cs.LG]

[39] Thomas A. Henzinger, Mathias Lechner, and Đorđe Žikelić. 2020. Scalable Verification of Quantized Neural Networks (Technical Report). arXiv:2012.08185

[40] Chao Huang, Jiameng Fan, Xin Chen, Wenchao Li, and Qi Zhu. 2020. Divide and Slide: Layer-Wise Refinement for Output Range Analysis of Deep Neural Networks. *IEEE Transactions on Computer-Aided Design of Integrated Circuits and Systems* 39, 11 (Nov. 2020), 3323–3335. <https://doi.org/10.1109/tcad.2020.3013071>

[41] Chao Huang, Jiameng Fan, Wenchao Li, Xin Chen, and Qi Zhu. 2019. ReachNN: Reachability Analysis of Neural-Network Controlled Systems. *ACM Transactions on Embedded Computing Systems* 18, 5s (Oct. 2019), 1–22. <https://doi.org/10.1145/3358228>

[42] Xiaowei Huang, Daniel Kroening, Wenjie Ruan, James Sharp, Youcheng Sun, Emese Thamo, Min Wu, and Xinping Yi. 2020. A survey of safety and trustworthiness of deep neural networks: Verification, testing, adversarial attack and defence, and interpretability. *Computer Science Review* 37 (2020), 100270. <https://doi.org/10.1016/j.cosrev.2020.100270>

[43] Xiaowei Huang, Marta Kwiatkowska, Sen Wang, and Min Wu. 2017. Safety verification of deep neural networks. In *Computer Aided Verification*. Springer, 3–29.

[44] Itay Hubara, Matthieu Courbariaux, Daniel Soudry, Ran El-Yaniv, and Yoshua Bengio. 2016. Binarized Neural Networks. In *Advances in Neural Information Processing Systems*, D. Lee, M. Sugiyama, U. Luxburg, I. Guyon, and R. Garnett (Eds.), Vol. 29. Curran Associates, Inc. <https://proceedings.neurips.cc/paper/2016/file/d8330f857a17c53d217014ee776bfd50-Paper.pdf>

[45] Itay Hubara, Matthieu Courbariaux, Daniel Soudry, Ran El-Yaniv, and Yoshua Bengio. 2017. Quantized Neural Networks: Training Neural Networks with Low Precision Weights and Activations. *J. Mach. Learn. Res.* 18, 1 (Jan. 2017), 6869–6898.

[46] Radoslav Ivanov, Taylor J. Carpenter, James Weimer, Rajeev Alur, George J. Pappas, and Insup Lee. 2021. Verifying the Safety of Autonomous Systems with Neural Network Controllers. *ACM Transactions on Embedded Computing Systems* 20, 1 (Jan. 2021), 1–26. <https://doi.org/10.1145/3419742>

[47] Kai Jia and Martin Rinard. 2020. Exploiting Verified Neural Networks via Floating Point Numerical Error. arXiv:2003.03021 [cs.LG]

[48] Robin Jia, Aditi Raghunathan, Kerem Göksel, and Percy Liang. 2019. Certified Robustness to Adversarial Word Substitutions. In *Proceedings of the 2019 Conference on Empirical Methods in Natural Language Processing and the 9th International Joint Conference on Natural Language Processing (EMNLP-IJCNLP)*. Association for Computational Linguistics, Hong Kong, China, 4129–4142. <https://doi.org/10.18653/v1/D19-1423>

[49] Guy Katz, Clark Barrett, David Dill, Kyle Julian, and Mykel Kochenderfer. 2017. Reluplex: An efficient SMT solver for verifying deep neural networks. In *Computer Aided Verification*. Springer, 97–117.

[50] Guy Katz, Derek A. Huang, Duligun Ibeling, Kyle Julian, Christopher Lazarus, Rachel Lim, Parth Shah, Shantanu Thakoor, Haoze Wu, Aleksandar Zelić, David L. Dill, Mykel J. Kochenderfer, and Clark Barrett. 2019. The Marabou Framework for Verification and Analysis of Deep Neural Networks. In *Computer Aided Verification*. Springer, 443–452. https://doi.org/10.1007/978-3-030-25540-4_26

[51] Yong-Deok Kim, Eunhyeok Park, Sungjoo Yoo, Taelim Choi, Lu Yang, and Dongjun Shin. 2016. Compression of Deep Convolutional Neural Networks for Fast and Low Power Mobile Applications. In *4th International Conference on Learning Representations, ICLR 2016, San Juan, Puerto Rico, May 2-4, 2016, Conference Track Proceedings*, Yoshua Bengio and Yann LeCun (Eds.). <http://arxiv.org/abs/1511.06530>

[52] Daniel Kroening and Michael Tautschnig. 2014. CBMC – C Bounded Model Checker. In *Tools and Algorithms for the Construction and Analysis of Systems*, Erika Ábrahám and Klaus Havelund (Eds.). Springer Berlin Heidelberg, Berlin, Heidelberg, 389–391.

[53] Y. Lecun, L. Bottou, Y. Bengio, and P. Haffner. 1998. Gradient-based learning applied to document recognition. *Proc. IEEE* 86, 11 (1998), 2278–2324. <https://doi.org/10.1109/5.726791>

[54] Darryl Lin, Sachin Talathi, and Sreekanth Annapureddy. 2016. Fixed Point Quantization of Deep Convolutional Networks. In *Proceedings of The 33rd International Conference on Machine Learning (Proceedings of Machine Learning Research, Vol. 48)*, Maria Florina Balcan and Kilian Q. Weinberger (Eds.). PMLR, New York, New York, USA, 2849–2858. <http://proceedings.mlr.press/v48/linb16.html>

[55] Changliu Liu, Tomer Arnon, Christopher Lazarus, Christopher Strong, Clark Barrett, and Mykel J. Kochenderfer. 2021. Algorithms for Verifying Deep Neural Networks. *Foundations and Trends in Optimization* 4, 3-4 (2021), 244–404. <https://doi.org/10.1561/2400000035>

[56] Scott Lundberg and Su-In Lee. 2017. A Unified Approach to Interpreting Model Predictions. In *Advances in Neural Information Processing Systems 30*, I. Guyon, U. Luxburg, S. Bengio, H. Wallach, R. Fergus, S. Vishwanathan, and R. Garnett (Eds.). Curran Associates, Inc., 4765–4774.

[57] Felipe Monteiro, Erickson Alves, Isabela Silva, Hussama Ismail, Lucas Cordeiro, and Eddie de Lima-Filho. 2018. ESBMC-GPU A context-bounded model checking tool to verify CUDA programs. *Science of Computer Programming* 152 (2018), 63–69.

[58] Ramon E. Moore, R. Baker Kearfott, and Michael J. Cloud. 2009. *Introduction to Interval Analysis*. Society for Industrial and Applied Mathematics, USA.

[59] Jeremy Morse, Mikhail Ramalho, Lucas C. Cordeiro, Denis A. Nicole, and Bernd Fischer. 2014. ESBMC 1.22 - (Competition Contribution). In *20th International Conference on Tools and Algorithms for the Construction and Analysis of Systems (TACAS) (LNCS, Vol. 8413)*. 405–407.

[60] Vinod Nair and Geoffrey E. Hinton. 2010. Rectified Linear Units Improve Restricted Boltzmann Machines (ICML’10). Omnipress, Madison, WI, USA, 807–814.

[61] Nina Narodytska, Shiva Kasiviswanathan, Leonid Ryzhyk, Mooly Sagiv, and Toby Walsh. 2018. Verifying Properties of Binarized Deep Neural Networks. <https://aaai.org/ocs/index.php/AAAI/AAAI18/paper/view/16898>

[62] Majid Nour, Zafer Cömert, and Kemal Polat. 2020. A Novel Medical Diagnosis model for COVID-19 infection detection based on Deep Features and Bayesian Optimization. *Applied Soft Computing* 97 (Dec. 2020), 106580. <https://doi.org/10.1016/j.asoc.2020.106580>

[63] Giambattista Parascandolo, Heikki Huttunen, and Tuomas Virtanen. 2016. Taming the waves: sine as activation function in deep neural networks. (2016).

[64] Adam Paszke, Sam Gross, Francisco Massa, Adam Lerer, James Bradbury, Gregory Chanan, Trevor Killeen, Zeming Lin, Natalia Gimelshein, Luca Antiga, et al. 2019. Pytorch: An imperative style, high-performance deep learning library. *arXiv preprint arXiv:1912.01703* (2019).

[65] Luca Pulina and Armando Tacchella. 2012. Challenging SMT solvers to verify neural networks. *Ai Communications* 25, 2 (2012), 117–135.

[66] Mohammad Rastegari, Vicente Ordóñez, Joseph Redmon, and Ali Farhadi. 2016. XNOR-Net: ImageNet Classification Using Binary Convolutional Neural Networks. In *Computer Vision – ECCV 2016*, Bastian Leibe, Jiri Matas, Nicu Sebe, and Max Welling (Eds.). Springer International Publishing, Cham, 525–542.

[67] Williame Rocha, Herbert Rocha, Hussama Ismail, Lucas Cordeiro, and Bernd Fischer. 2017. DepthK: A k-Induction Verifier Based on Invariant Inference for C Programs - (Competition Contribution). In *26th International Conference on Tools and Algorithms for the Construction and Analysis of Systems*. 360–364.

[68] Ansgar Rössig and Milena Petkovic. 2020. Advances in verification of ReLU neural networks. *Journal of Global Optimization* (Oct. 2020). <https://doi.org/10.1007/s10898-020-00949-1>

[69] Luiz Sena, Iury Bessa, Mikhail Ramalho, Lucas Cordeiro, and Edjard Mota. 2019. Incremental Bounded Model Checking of Artificial Neural Networks in CUDA. In *IX Brazilian Symposium on Computing Systems Engineering*.

[70] Gagandeep Singh, Timon Gehr, Matthew Mirman, Markus Püschel, and Martin T Vechev. 2018. Fast and Effective Robustness Certification. *NeurIPS* 1, 4 (2018), 6.

[71] Vincent Sitzmann, Julien Martel, Alexander Bergman, David Lindell, and Gordon Wetzstein. 2020. Implicit neural representations with periodic activation functions. *Advances in Neural Information Processing Systems* 33 (2020).

[72] Youcheng Sun, Xiaowei Huang, Daniel Kroening, James Sharp, Matthew Hill, and Rob Ashmore. 2019. Structural Test Coverage Criteria for Deep Neural Networks. *ACM Transactions on Embedded Computing Systems* 18, 5s (Oct. 2019), 1–23. <https://doi.org/10.1145/3358233>

[73] Christian Szegedy, Wojciech Zaremba, Ilya Sutskever, Joan Bruna, Dumitru Erhan, Ian Goodfellow, and Rob Fergus. 2014. Intriguing properties of neural networks. In *International Conference on Learning Representations*. <http://arxiv.org/abs/1312.6199>

[74] Vincent Tjeng, Kai Y. Xiao, and Russ Tedrake. 2019. Evaluating Robustness of Neural Networks with Mixed Integer Programming. In *International Conference on Learning Representations*.

[75] Hoang-Dung Tran, Xiaodong Yang, Diego Manzanas Lopez, Patrick Musau, Luan Viet Nguyen, Weiming Xiang, Stanley Bak, and Taylor T. Johnson. 2020. NNV: The Neural Network Verification Tool for Deep Neural Networks and Learning-Enabled Cyber-Physical Systems. In *Computer Aided Verification*. Springer, 3–17. https://doi.org/10.1007/978-3-030-53288-8_1

[76] Andreas Venzke and Spyros Chatzivasileiadis. 2021. Verification of Neural Network Behaviour: Formal Guarantees for Power System Applications. *IEEE Transactions on Smart Grid* 12, 1 (Jan. 2021), 383–397. <https://doi.org/10.1109/tsg.2020.3009401>

[77] Yakir Vizel, Georg Weissenbacher, and Sharad Malik. 2015. Boolean Satisfiability Solvers and Their Applications in Model Checking. *Proc. IEEE* 103, 11 (2015), 2021–2035. <https://doi.org/10.1109/JPROC.2015.2455034>

- [78] Shiqi Wang, Kexin Pei, Justin Whitehouse, Junfeng Yang, and Suman Jana. 2018. Efficient Formal Safety Analysis of Neural Networks. In *Proceedings of the 32nd International Conference on Neural Information Processing Systems* (Montréal, Canada). Curran Associates Inc., 6369–6379.
- [79] Huihui Wu, Deyun Lv, Tengxiang Cui, Gang Hou, Masahiko Watanabe, and Weiqiang Kong. 2021. SDLV: Verification of Steering Angle Safety for Self-Driving Cars. *Formal Aspects of Computing* (March 2021). <https://doi.org/10.1007/s00165-021-00539-2>
- [80] Zonghan Wu, Shirui Pan, Fengwen Chen, Guodong Long, Chengqi Zhang, and Philip S. Yu. 2021. A Comprehensive Survey on Graph Neural Networks. *IEEE Transactions on Neural Networks and Learning Systems* 32, 1 (2021), 4–24. <https://doi.org/10.1109/TNNLS.2020.2978386>
- [81] Weiming Xiang, Hoang-Dung Tran, and Taylor T. Johnson. 2018. Output Reachable Set Estimation and Verification for Multilayer Neural Networks. *IEEE Transactions on Neural Networks and Learning Systems* 29, 11 (Nov. 2018), 5777–5783. <https://doi.org/10.1109/tnnls.2018.2808470>